PHYSICAL REVIEW C **91**, 025501 (2015)

Superallowed $0^+ \rightarrow 0^+$ nuclear β decays: 2014 critical survey, with precise results for V_{ud} and CKM unitarity

J. C. Hardy* and I. S. Towner†
Cyclotron Institute, Texas A&M University, College Station, Texas 77843, USA
(Received 21 November 2014; published 12 February 2015)

A new critical survey is presented of all half-life, decay-energy, and branching-ratio measurements related to 20 superallowed $0^+ \rightarrow 0^+ \beta$ decays. Included are 222 individual measurements of comparable precision obtained from 177 published references. Compared with our last review in 2008, we have added results from 24 new publications and eliminated 9 references, the results from which having been superseded by much more precise modern data. We obtain world-average ft values for each of the 18 transitions that have a complete set of data, then apply radiative and isospin-symmetry-breaking corrections to extract "corrected" $\mathcal{F}t$ values. Fourteen of these $\mathcal{F}t$ values now have a precision of order 0.1% or better. In the process of obtaining these results we carefully evaluate the available calculations of the isospin-symmetry-breaking corrections by testing the extent to which they lead to $\mathcal{F}t$ values consistent with conservation of the vector current. Only one set of calculations satisfactorily meets this condition. The resultant average $\mathcal{F}t$ value, when combined with the muon lifetime, yields the up-down quark-mixing element of the Cabibbo-Kobayashi-Maskawa matrix, $V_{ud} = 0.974\,17 \pm 0.000\,21$. The unitarity test on the top row of the matrix becomes $|V_{ud}|^2 + |V_{us}|^2 + |V_{ub}|^2 = 0.999\,78 \pm 0.000\,55$ if the Particle Data Group (PDG) recommended value for V_{us} is used. However, recent lattice QCD calculations, not included yet in the PDG evaluation, have introduced some inconsistency into kaon-decay measurements of V_{us} and V_{us}/V_{ud}. We examine the impact of these new results on the unitarity test and conclude that there is no evidence of any statistically significant violation of unitarity. Finally, from the $\mathcal{F}t$-value data we also set limits on the possible existence of scalar interactions.

DOI: 10.1103/PhysRevC.91.025501 PACS number(s): 23.40.Bw, 12.15.Hh, 12.60.−i

I. INTRODUCTION

Precise measurements of the β decay between nuclear analog states of spin, $J^\pi = 0^+$, and isospin, $T = 1$, provide demanding and fundamental tests of the properties of the electroweak interaction. Collectively, these transitions sensitively probe the conservation of the vector weak current, set tight limits on the presence of scalar currents, and provide the most precise value for V_{ud}, the up-down quark-mixing element of the Cabibbo-Kobayashi-Maskawa (CKM) matrix. This latter result has become a linchpin in the most demanding available test of the unitarity of the CKM matrix, a property which is fundamental to the electroweak standard model.

We have published six previous surveys of $0^+ \rightarrow 0^+$ superallowed transitions [1–6], the first having appeared over 40 years ago and the most recent 6 years ago. In each, we published a complete survey of all relevant nuclear data that pertained to these superallowed transitions and used the results to set limits on the weak-interaction parameters that were important at the time. Notably, since V_{ud} became the quantity of greatest interest 25 years ago, its value as obtained from our surveys of superallowed decays has improved by a factor of five in precision but has never strayed outside of the uncertainties quoted in preceding surveys. This consistency is testimony to the robustness of what is by now a very large body of nuclear data.

Since our last survey closed in September 2008, there has continued to be a great deal of activity in this field, both in experiment and in theory. This activity in honing V_{ud} has been matched by efforts to make similar improvements in the value of V_{us}, the second important element in the top-row unitarity sum. (The third element, V_{ub}, is too small to play a significant role.) Because the value of V_{us} has undergone some unexpected changes in the past decade and has not yet settled at a reliably stable result, interest in the CKM unitarity test continues to stimulate work in the field. Since 2008, new measurements relating to $0^+ \rightarrow 0^+$ superallowed transitions have appeared in 24 publications, and the new more-precise results they contain have made 9 of the references accumulated in 2008 entirely obsolete and left 11 more with some results replaced, in all cases because new values had uncertainties a factor of ten or more smaller. Altogether, this means that, of the references in this 2014 survey, about 15% are new and, being among the most precise, their influence is disproportionately greater than that.

In addition to new measurements, there have also been important theoretical contributions to the small isospin-symmetry-breaking corrections that must be applied to the data to extract V_{ud} and the values of other weak-interaction parameters. In the past 6 years, a number of different groups have published their results for these terms, with calculations based upon a variety of different models. The diversity of results has prompted development of a test that allows each set of correction terms to be judged by its ability to produce $\mathcal{F}t$ values that are consistent with conservation of the vector current (CVC). As part of our survey, we apply this test to all sets that cover at least half the number of well-measured

*hardy@comp.tamu.edu
†towner@comp.tamu.edu

superallowed transitions. As a result, we have identified the only set that yields self-consistent $\mathcal{F}t$ values and it is this set that we use in our ultimate analysis of the experimental data.

Overall, recent improvements have been numerous enough that we consider this to be an opportune time to produce a new and updated survey of the nuclear data used to establish V_{ud}. We incorporate data on a total of 20 superallowed transitions and have continued the practice we began in 1984 [3] of updating all original data to take account of the most modern calibration standards. However, many of the measurements that required updating have been superseded by more precise modern measurements so there are fewer updated old results in our new survey than there have been in the past.

Superallowed $0^+ \rightarrow 0^+ \beta$ decay between $T = 1$ analog states depends uniquely on the vector part of the weak interaction and, according to the CVC hypothesis, its experimental ft value should be directly related to the vector coupling constant, a fundamental constant which is the same for all such transitions. In practice, the expression for ft includes several small ($\sim$1%) correction terms. It is convenient to combine some of these terms with the ft value and define a "corrected" $\mathcal{F}t$ value. Thus, we write [6]

$$\mathcal{F}t \equiv ft(1+\delta_R')(1+\delta_{\rm NS}-\delta_C) = \frac{K}{2G_{\rm V}^2\left(1+\Delta_{\rm R}^{\rm V}\right)}, \qquad (1)$$

where $K/(\hbar c)^6 = 2\pi^3\hbar \ln 2/(m_e c^2)^5 = 8120.2776(9) \times 10^{-10}$ GeV^{-4} s, $G_{\rm V}$ is the vector coupling constant for semileptonic weak interactions, δ_C is the isospin-symmetry-breaking correction, and $\Delta_{\rm R}^{\rm V}$ is the transition-independent part of the radiative correction. The terms δ_R' and $\delta_{\rm NS}$ comprise the transition-dependent part of the radiative correction, the former being a function only of the electron's energy and the Z of the daughter nucleus, while the latter, like δ_C, depends in its evaluation on the details of nuclear structure. From this equation, it can be seen that each measured transition establishes an individual value for $G_{\rm V}$ and, if the CVC assertion is correct that $G_{\rm V}$ is not renormalized in the nuclear medium, all such values—and all the $\mathcal{F}t$ values themselves—should be identical within uncertainties, regardless of the specific nuclei involved.

Our procedure in this paper is to examine all experimental data related to 20 superallowed transitions, comprising all those that have been well studied, together with other cases that are now coming under scrutiny after becoming accessible to precision measurement in relatively recent years. The methods used in data evaluation are presented in Sec. II, with the calculations and corrections required to extract $\mathcal{F}t$ values from these data being described and applied in Sec. III. Then in Sec. IV we take a careful look at the various sets of isospin-symmetry-breaking correction terms and explain our choice of the set we use for the survey results. Finally, in Sec. V we explore the impact of these results on two weak-interaction issues: CKM unitarity and the possible existence of scalar interactions. This is much the same pattern as we followed in our last two reviews [5,6] so we do not describe the formalism again in detail, referring the reader instead to those earlier works.

II. EXPERIMENTAL DATA

The ft value that characterizes any β transition depends on three measured quantities: the total transition energy $Q_{\rm EC}$, the half-life $t_{1/2}$ of the parent state, and the branching ratio R for the particular transition of interest. The $Q_{\rm EC}$ value is required to determine the statistical rate function, f, while the half-life and branching ratio combine to yield the partial half-life, t. In Tables I–VII we present the measured values of these three quantities and supporting information for a total of 20 superallowed transitions. In all, there are 222 independent measurements from 177 references. Thus, on average, each quantity has been measured with comparable precision three or more times by different groups. Such redundancy virtually eliminates the possibility of individual experimental anomalies having a significant impact on the overall results.

A. Evaluation principles

In our treatment of the data, we considered all measurements formally published before September 2014. We scrutinized all the original experimental reports in detail. Where necessary and possible, we used the information provided there to correct the results for calibration data that have improved since the measurement was made. If corrections were evidently required but insufficient information was provided to make them, the results were rejected. Of the surviving results, only those with (updated) uncertainties that are within a factor of ten of the most precise measurement for each quantity were retained for averaging in the tables. Each datum appearing in the tables is attributed to its original journal reference *via* an alphanumeric code comprising the initial two letters of the first author's name and the two last digits of the publication date. These codes are correlated with the actual reference numbers, Refs. [7]–[184], in Table VIII.

The statistical procedures we have followed in analyzing the tabulated data are based on those used by the Particle Data Group in their periodic reviews of particle properties (e.g., Ref. [185]) and adopted by us in our previous surveys. We gave a detailed description of those procedures in our 2004 survey [5] so do not repeat it here.

Our evaluation principles and associated statistical procedures constitute a very conservative approach to the data. Unless there is a clearly identifiable reason to reject a result, we include it in our database even if it deviates significantly from other measurements of the same quantity, the consequent nonstatistical spread in results being reflected in an increased uncertainty assigned to the average. Wherever this occurs, the factor by which the uncertainty has been increased, which is the square root of the normalized χ^2, is listed in the "scale" column of a table. Occasionally a measurement with an acceptable uncertainty is nevertheless excluded from our database, in which case the reason for its exclusion is always listed in Table VII. For example, there are a few publications that include a number of measurements—a set of half-lives or $Q_{\rm EC}$ values—most or all of which deviate substantially from other accepted measurements of the same quantities. In those cases, we consider that some systematic problem has been revealed and exclude all the results from that publication.

TABLE I. Measured results from which the decay transition energies, Q_{EC}, have been derived for superallowed β decays. The lines giving the average superallowed Q_{EC} values themselves are in bold print. (See Table VIII for the correlation between the alphanumeric reference code used in this table and the actual reference numbers.)

Parent/daughter property[a]			Measured energies used to determine Q_{EC} (keV)			Average value	
Nuclei			1	2	3	Energy (keV)	Scale
$T_z = -1$							
^{10}C	^{10}B	Q_{EC}(gs)	3647.83 ± 0.34 [Ba84]	3647.95 ± 0.12 [Ba98]	3648.12 ± 0.08 [Er11]		
			3648.34 ± 0.51 [Kw13]			3648.063 ± 0.064	1.0
		$E_x(d0^+)$	1740.15 ± 0.17 [Aj88]	1740.068 ± 0.017[b]		1740.069 ± 0.017	1.0
		Q_{EC}(sa)				**1907.994** ± 0.067	
^{14}O	^{14}N	Q_{EC}(gs)	5143.30 ± 0.60 [Bu61]	5145.05 ± 0.46 [Ba62]	5145.52 ± 0.48 [Ro70]		
			5143.43 ± 0.37 [Wh77]	5144.33 ± 0.17 [To03]		5144.32 ± 0.28	2.1
		$E_x(d0^+)$	2312.798 ± 0.011 [Aj91]			2312.798 ± 0.011	
		Q_{EC}(sa)				**2831.23** ± 0.23[c]	**2.3**
^{18}Ne	^{18}F	ME(p)	5316.8 ± 1.5 [Ma94]	5317.63 ± 0.36 [Bl04b]		5317.58 ± 0.35	1.0
		ME(d)	871.99 ± 0.73 [Bo64]	874.2 ± 2.2 [Ho64]	875.2 ± 2.8 [Pr67]		
			877.2 ± 3.0 [Se73]	874.01 ± 0.60 [Ro75]		873.37 ± 0.59	1.3
		Q_{EC}(gs)				4444.21 ± 0.68	
		$E_x(d0^+)$	1041.55 ± 0.08 [Ti95]			1041.55 ± 0.08	
		Q_{EC}(sa)				**3402.66** ± 0.69	
^{22}Mg	^{22}Na	ME(p)	−401.2 ± 3.0 [Ha74c]	−400.8 ± 1.2[d]	−400.5 ± 1.0 [Pa05]	−400.67 ± 0.73	1.0
		ME(d)	−5184.3 ± 1.5 [We68]	−5182.5 ± 0.5 [Be68]	−5181.3 ± 1.7 [An70]		
			−5183.2 ± 1.0 [Gi72]	−5181.56 ± 0.16 [Mu04]	−5181.08 ± 0.30 [Sa04]	−5181.58 ± 0.23	1.7
		Q_{EC}(gs)	4781.64 ± 0.28 [Mu04]	4781.40 ± 0.67 [Sa04]		4781.53 ±0.24	1.0
		$E_x(d0^+)$	657.00 ± 0.14 [En98]			657.00 ± 0.14	
		Q_{EC}(sa)				**4124.53** ± 0.28	
^{26}Si	^{26}Al	ME(p)	−7145.4 ± 3.0 [Ha74c]	−7139.5 ± 1.0 [Pa05]	−7140.4 ± 2.9 [Kw10]	−7140.1 ± 1.2	1.3
		ME($d0^+$)	−11 981.96 ± 0.26[e]			−11 981.96 ± 0.26	
		Q_{EC}(sa)	4840.85 ± 0.10 [Er09a]			**4840.86** ± 0.10	**1.0**
^{30}S	^{30}P	ME(p)	−14 060 ± 15 [Mi67]	−14 054 ± 25 [Mc67]	−14 068 ± 30 [Ha68]		
			−14 063.4 ± 3.0 [Ha74c]			−14 063.1 ± 2.9	1.0
		ME(d)	−20 203 ± 3 [Ha67]	−20 200.61 ± 0.40 [Re85]		−20 200.65 ± 0.40	1.0
		Q_{EC}(gs)	6141.61 ± 0.19 [So11]			6141.59 ± 0.26	1.4
		$E_x(d0^+)$	677.29 ± 0.07 [En98]			677.29 ± 0.07	
		Q_{EC}(sa)				**5464.30** ± 0.27	
^{34}Ar	^{34}Cl	ME(p)	−18 380.2 ± 3.0 [Ha74c]	−18 378.4 ± 3.5 [He01]	−18 377.10 ± 0.41 [He02]	−18 377.17 ± 0.40	1.0
		ME(d)	−24 440.03 ± 0.06[e]			−24 440.03 ± 0.06	
		Q_{EC}(sa)	6061.83 ± 0.08 [Er11]			**6061.87** ± 0.19	**2.5**
^{38}Ca	^{38}K	ME(p)	−22 058.53 ± 0.28 [Ri07]	−22 058.01 ± 0.65 [Ge07]		−22 058.45 ± 0.26	1.0
		ME($d0^+$)	−28 670.58 ± 0.21[e]			−28 670.58 ± 0.21	
		Q_{EC}(sa)	6612.12 ± 0.07 [Er11]			**6612.12** ± 0.07	**1.0**
^{42}Ti	^{42}Sc	**Q_{EC}(sa)**	7016.83 ± 0.25 [Ku09]			**7016.83** ± 0.25	
$T_z = 0$							
^{26m}Al	^{26}Mg	Q_{EC}(gs)	4004.79 ± 0.55 [De69]	4004.41 ± 0.10[f]	4004.37 ± 0.22 [Ge08]	4004.41 ± 0.09	1.0
		$E_x(p0^+)$	228.305 ± 0.013 [En98]			228.305 ± 0.013	
		Q_{EC}(sa)	4232.19 ± 0.12 [Br94]	4232.83 ± 0.13 [Er06b]		**4232.66** ± 0.12[c]	**2.1**
^{34}Cl	^{34}S	**Q_{EC}(sa)**	5491.65 ± 0.26[g]	5491.662 ± 0.047 [Er09b]		**5491.662** ± 0.046	**1.0**
^{38m}K	^{38}Ar	**Q_{EC}(sa)**	6044.38 ± 0.12 [Ha98]	6044.223 ± 0.041 [Er09b]		**6044.240** ± 0.048	**1.2**
^{42}Sc	^{42}Ca	**Q_{EC}(sa)**	6425.84 ± 0.17[h]	6426.13 ± 0.21 [Er06b]		**6426.28** ± 0.30[c]	**3.0**
^{46}V	^{46}Ti	**Q_{EC}(sa)**	7052.90 ± 0.40 [Sa05]	7052.72 ± 0.31 [Er06b]	7052.11 ± 0.27 [Fa09]		
			7052.44 ± 0.10 [Er11]			**7052.45** ± 0.10	**1.1**
^{50}Mn	^{50}Cr	**Q_{EC}(sa)**	7634.48 ± 0.07 [Er08]			**7634.451** ± 0.066[c]	**1.0**
^{54}Co	^{54}Fe	**Q_{EC}(sa)**	8244.54 ± 0.10 [Er08]			**8244.37** ± 0.28[c]	**3.4**
^{62}Ga	^{62}Zn	**Q_{EC}(sa)**	9181.07 ± 0.54 [Er06a]			**9181.07** ± 0.54	
^{66}As	^{66}Ge	ME(p)	−52018 ± 30 [Sc07]			−52018 ± 30	
		ME(d)	−61 607.0 ± 2.4 [Sc07]			−61 607.0 ± 2.4	
		Q_{EC}(sa)	9550 ± 50 [Da80]			**9579** ± 26	**1.0**
^{70}Br	^{70}Se	**Q_{EC}(sa)**	9970 ± 170 [Da80]			**9970** ± 170	

TABLE I. (*Continued.*)

Parent/daughter property[a]			Measured energies used to determine Q_{EC} (keV)			Average value	
Nuclei			1	2	3	Energy (keV)	Scale
^{74}Rb	^{74}Kr	ME(p)	−51 905 ± 18 [He02]	−51 915.2 ± 4.0 [Ke07]	−51 916.5 ± 6.0 [Et11]	−51 915.2 ± 3.3	1.0
		ME(d)	−62 332.0 ± 2.1 [Ro06]			−62 332.0 ± 2.1	
		Q_{EC}(sa)				**10 416.8** ± 3.9	

[a]Abbreviations used in this column are as follows: "gs", transition between ground states; "sa", superallowed transition; "p", parent; "d", daughter; "ME", mass excess; "$E_x(0^+)$", excitation energy of the 0^+ (analog) state. Thus, for example, "Q_{EC}(sa)" signifies the Q_{EC} value for the superallowed transition, "ME(d)", the mass excess of the daughter nucleus; and "ME($d0^+$), the mass excess of the daughter's 0^+ state.
[b]Result based on Refs. [Ba88] and [Ba89].
[c]Average result includes the results of Q_{EC} pairs; see Table II.
[d]Result based on Refs. [Bi03], [Se05], and [Je07].
[e]Result obtained from the Q_{EC} value for the superallowed decay of $d0^+$, which appears elsewhere in this table, combined with the mass of its daughter taken from Ref. [Wa12].
[f]Result based on Refs. [Is80], [Al82], [Hu82], [Be85], [Pr90], [Ki91], and [Wa92].
[g]Result based on Refs. [Wa83], [Ra83], and [Li94].
[h]Result based on Refs. [Zi87] and [Ki89].

B. Data tables

The Q_{EC}-value data appear in Tables I and II. Of the 20 superallowed decays listed, nine—those of ^{10}C, ^{14}O, ^{26}Al^m, ^{34}Cl, ^{38}K^m, ^{42}Sc, ^{46}V, ^{50}Mn, and ^{54}Co—have stable daughter nuclei. In past surveys, the corresponding Q_{EC} values were predominantly obtained from direct reaction measurements but, by now, all but the ^{14}O Q_{EC} value have been measured with a Penning trap. Each of these latter measurements has determined the parent and daughter masses interleaved in a single experiment, thus effectively measuring the Q_{EC} value directly from the ratio of cyclotron frequencies. All direct measurements of a Q_{EC} value are identified in column 3 of Table I by "Q_{EC}(sa)" and each individual result, whether reaction or Penning-trap based, is itemized with its appropriate reference in the next three columns. The weighted average of all measurements for a particular decay appears in column 7, with the corresponding scale factor (see Sec. II A) in column 8. Four of these cases, ^{10}C, ^{34}Cl, ^{38}K^m, and ^{46}V, have no further complications. For the remaining five, however, in addition to the individual Q_{EC}-value results, Q_{EC}-value differences have also been obtained via (^{3}He, t) reactions on composite targets. These difference measurements are presented in Table II. They have been dealt with in combination with the direct Q_{EC}-value measurements to obtain a best overall fit by a method described in our 2004 survey [5]. The final average Q_{EC} value for each transition appears in column 7 of Table I and the average differences are in column 4 of Table II. All are flagged with footnotes to indicate the interconnection.

TABLE II. Q_{EC}-value differences for superallowed β-decay branches. These data are also used as input to determine some of the average Q_{EC} values listed in Table I. (See Table VIII for the correlation between the alphabetical reference code used in this table and the actual reference numbers.)

Parent nucleus 1	Parent nucleus 2	$Q_{EC2} - Q_{EC1}$ (keV)	
		Measurement	Average[a]
^{14}O	^{26m}Al	1401.68 ± 0.13 [Ko87]	1401.43 ± 0.26
^{26m}Al	^{42}Sc	2193.5 ± 0.2 [Ko87]	2193.62 ± 0.32
^{42}Sc	^{50}Mn	1207.6 ± 2.3 [Ha74d]	1208.17 ± 0.31
^{42}Sc	^{54}Co	1817.2 ± 0.2 [Ko87]	1818.10 ± 0.41
^{50}Mn	^{54}Co	610.09 ± 0.17 [Ko87] [Ko97b]	609.92 ± 0.29

[a]Average values include the results of direct Q_{EC}-value measurements: see Table I.

There are two cases, ^{26}Al^m and ^{38}K^m, in which the superallowed decay originates from an isomeric state. For the former, there are Q_{EC}-value measurements of comparable precision that correspond to the ground state as well as to the isomer. Obviously, the two sets of measurements are simply related to one another by the excitation energy of the isomeric state in the parent. In Table I the set of measurements for the ground-state Q_{EC} value and for the excitation energy of the isomeric state appear in separate rows, each with its identifying property given in column 3 and its weighted average appearing in column 7. In the row below, the average value given in column 7 for the superallowed transition is the weighted average not only of the direct superallowed Q_{EC}-value measurements in that row, but also of the result derived from the two preceding rows. Note that in all cases the Q_{EC} value for the superallowed transition appears in boldface type.

For the remaining transitions, those which have unstable parents and daughters, the situation is somewhat more complicated. In some cases only the parent and daughter masses have been measured, either from transfer reactions or by Penning trap, but not the Q_{EC} value. In other cases, the measured results for masses and Q_{EC} values are of comparable precision and so both must be included in the average. Also, in most of the cases with $T_Z = -1$ parents, the masses of the parent and daughter nuclei are not sufficient to determine the Q_{EC} value for the superallowed branch; that also requires the excitation energy of the analog 0^+ state in the daughter. If needed, all of these properties are identified in column 3 of Table I, with the individual measurements of that property, their weighted average, and a scale factor appearing in columns to the right. The average Q_{EC} value listed for the corresponding superallowed transition is obtained from these separate averages and appears in bold print.

TABLE III. Half-lives, $t_{1/2}$, of superallowed β emitters. (See Table VIII for the correlation between the alphabetical reference code used in this table and the actual reference numbers.)

Parent nucleus	Measured half-lives, $t_{1/2}$ (ms)				Average value	
	1	2	3	4	$t_{1/2}$ (ms)	Scale
$T_z = -1$						
^{10}C	19 280 ± 20 [Az74]	19 295 ± 15 [Ba90]	19 310 ± 4 [Ia08]	19 282 ± 11 [Ba09]	19 305.2 ± 7.1	2.0
^{14}O	70 480 ± 150 [Al72]	70 588 ± 28 [Cl73]	70 430 ± 180 [Az74]	70 684 ± 77 [Be78]		
	70 613 ± 25 [Wi78]	70 560 ± 49 [Ga01]	70 641 ± 20 [Ba04]	70 696 ± 52 [Bu06]		
	70 623 ± 53 [Ta12]	70 610 ± 30 [La13]	70 632 ± 94 [La13]		70 619 ± 11	1.0
^{18}Ne	1669 ± 4 [Al75]	1687 ± 9 [Ha75]	1664.8 ± 1.1 [Gr13]		1665.4 ± 1.1	1.1
^{22}Mg	3857 ± 9 [Ha75]	3875.5 ± 1.2 [Ha03]			3875.2 ± 2.4	2.0
^{26}Si	2245.3 ± 0.7 [Ia10]				2245.3 ± 0.7	
^{30}S	1178.3 ± 4.8 [Wi80]	1175.9 ± 1.7 [So11]			1176.2 ± 1.6	1.0
^{34}Ar	844.5 ± 3.4 [Ha74a]	843.8 ± 0.4 [Ia06]			843.8 ± 0.4	1.0
^{38}Ca	443.8 ± 1.9 [Bl10]	443.77 ± 0.36 [Pa11]			443.77 ± 0.35	1.0
^{42}Ti	202 ± 5 [Ga69]	208.14 ± 0.45 [Ku09]			208.09 ± 0.55	1.2
$T_z = 0$						
^{26m}Al	6346 ± 5 [Fr69a]	6346 ± 5 [Az75]	6339.5 ± 4.5 [Al77]	6346.2 ± 2.6 [Ko83]		
	6346.54 ± 0.76 [Fi11]	6347.8 ± 2.5 [Sc11]	6345.3 ± 0.9 [Ch13]		6346.02 ± 0.54	1.0
^{34}Cl	1526 ± 2 [Ry73]	1525.2 ± 1.1 [Wi76]	1527.7 ± 2.2 [Ko83]	1526.8 ± 0.5 [Ia06]	1526.55 ± 0.44	1.0
^{38m}K	925.6 ± 0.7 [Sq75]	922.3 ± 1.1 [Wi76]	921.71 ± 0.65 [Wi78]	924.15 ± 0.31 [Ko83]		
	924.4 ± 0.6 [Ba00]	924.46 ± 0.14 [Ba10]			924.33 ± 0.27	2.3
^{42}Sc	680.98 ± 0.62 [Wi76]	680.67 ± 0.28 [Ko97a]			680.72 ± 0.26	1.0
^{46}V	422.47 ± 0.39 [Al77]	422.28 ± 0.23 [Ba77a]	422.57 ± 0.13 [Ko97a]	422.66 ± 0.06 [Pa12]	422.622 ± 0.053	1.2
^{50}Mn	284.0 ± 0.4 [Ha74b]	282.8 ± 0.3 [Fr75]	282.72 ± 0.26 [Wi76]	283.29 ± 0.08 [Ko97a]		
	283.10 ± 0.14 [Ba06]				283.21 ± 0.11	1.7
^{54}Co	193.4 ± 0.4 [Ha74b]	193.0 ± 0.3 [Ho74]	193.28 ± 0.18 [Al77]	193.28 ± 0.07 [Ko97a]	193.271 ± 0.063	1.0
^{62}Ga	115.84 ± 0.25 [Hy03]	116.19 ± 0.04 [Bl04a]	116.09 ± 0.17 [Ca05]	116.01 ± 0.19 [Hy05]		
	116.100 ± 0.025 [Gr08]				116.121 ± 0.040	1.9
^{66}As	95.78 ± 0.39 [Al78]	95.77 ± 0.28 [Bu88]	97 ± 2 [Ji02]		95.79 ± 0.23	1.0
^{70}Br	80.2 ± 0.8 [Al78]	78.54 ± 0.59 [Bu88]			79.12 ± 0.79	1.7
^{74}Rb	64.90 ± 0.09 [Oi01]	64.761 ± 0.031 [Ba01]			64.776 ± 0.043	1.5

As in our previous surveys, we have not used the current Atomic Mass Evaluation tables [176] to derive the Q_{EC} values of interest. Our method is to include all pertinent measurements for each property; typically, only a subset of the available data is included as input to the mass tables. Furthermore, we have examined each reference in detail and either accepted the result, updated it to modern calibration standards, or rejected it for cause. The updating procedures are outlined, reference by reference, in Table VI and the rejected results are similarly documented in Table VII. With a comparatively small data set, we could afford to pay the kind of individual attention that is impossible when one is considering all nuclear masses.

One of our omissions from Table I requires a more detailed explanation than could be included in Table VII. There are two reported measurements of the ^{70}Br Q_{EC} value. The first is a rather old result in Da80 [50], which came from a measurement of the positron end-point energy as recorded in a plastic scintillator; the second one was reported very recently in Sa09 [159] and is based on Penning-trap measurements. Since the latter's uncertainty is more than ten times smaller than the former's, it would normally be the only one to appear in our table. However, we have chosen to eliminate it and include only the old imprecise measurement. The reason is made clear in Fig. 1, where the Penning-trap result is seen to deviate from systematic behavior by some 500 keV. Penning

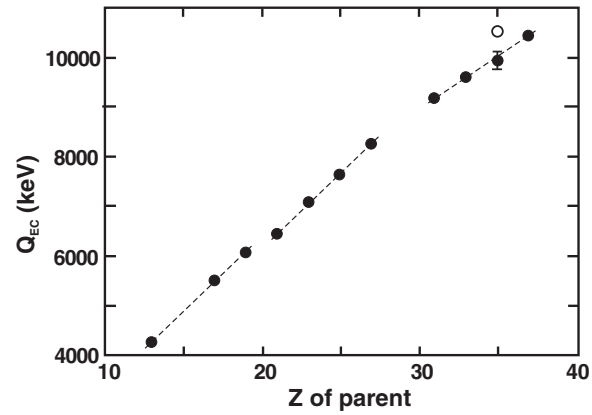

FIG. 1. The tabulated Q_{EC} values for the $T_Z = 0$ superallowed transitions in Table I (solid points) are plotted as a function of the Z of the parent nucleus. For all cases other than that of ^{70}Br the uncertainties are smaller than the plotted points. The open circle at $Z = 35$ is the Q_{EC} value measured by Penning trap [159] and assigned to the superallowed transition from ^{70}Br. As explained in the text and noted in Table VII, this result has been omitted from Table I. The dashed lines are only to guide the eye; separate straight lines are drawn for each of the sd, $f_{7/2}$, and upper-fp shells.

TABLE IV. Measured results from which the branching ratios, R, have been derived for superallowed β transitions. The lines giving the average superallowed branching ratios themselves are in bold print. (See Table VIII for the correlation between the alphabetical reference code used in this table and the actual reference numbers.)

Parent/daughter nuclei		Daughter state E_x (MeV)	Measured branching ratio, R (%) 1	2	Average value R (%)	Scale
$T_z = -1$						
^{10}C	^{10}B	2.16	$0^{+0.0008}_{-0}$ [Go72]		$0^{+0.0008}_{-0}$	
		1.74	1.468 ± 0.014 [Ro72]	1.473 ± 0.007 [Na91]		
			1.465 ± 0.009 [Kr91]	1.4625 ± 0.0025 [Sa95]		
			1.4665 ± 0.0038 [Fu99]		**1.4646 ± 0.0019**	**1.0**
^{14}O	^{14}N	gs	0.68 ± 0.10 [Sh55,To05]	0.74 ± 0.05 [Fr63,To05]		
			0.54 ± 0.02 [Si66,To05]		0.571 ± 0.068	3.7
		3.95	0.062 ± 0.007 [Ka69]	0.058 ± 0.004 [Wi80]		
			0.053 ± 0.002 [He81]		0.0545 ± 0.0019	1.1
		2.31			**99.374 ± 0.068**	
^{18}Ne	^{18}F	**1.04**	9 ± 3 [Fr63]	7.69 ± 0.21[a] [Ha75]	**7.70 ± 0.21**	**1.0**
^{22}Mg	^{22}Na	**0.66**	54.0 ± 1.1 [Ha75]	53.15 ± 0.12 [Ha03]	**53.16 ± 0.12**	**1.0**
^{26}Si	^{26}Al	1.06	21.8 ± 0.8 [Ha75]	21.21 ± 0.64 [Ma08]	21.44 ± 0.50	1.0
		0.23			**75.49 ± 0.57**[a]	
^{30}S	^{30}P	gs	20 ± 1 [Fr63]		20 ± 1	
		0.68			**77.4 ± 1.0**[a]	
^{34}Ar	^{34}Cl	0.67	2.49 ± 0.10 [Ha74a]		2.49 ± 0.10	
		gs			**94.45 ± 0.25**[a]	
^{38}Ca	^{38}K	**0.13**	77.28 ± 0.16 [Pa14]		**77.28 ± 0.16**	
^{42}Ti	^{42}Sc	0.61	56 ± 14 [Al69]	51.1 ± 1.1 [Ku09]	51.1 ± 1.1	1.0
		gs			**47.7 ± 1.3**[a]	
$T_z = 0$						
^{26m}Al	^{26}Mg	**gs**	>99.997 [Ki91]	>99.9985 [Fi12]	$\mathbf{100.0000^{+0}_{-0.0015}}$	
^{34}Cl	^{34}S	**gs**	>99.988 [Dr75]		$\mathbf{100.000^{+0}_{-0.012}}$	
^{38m}K	^{38}Ar	3.38	<0.0019 [Ha94]	<0.0008 [Le08]	$0.0000^{+0.0008}_{-0}$	
		gs(^{38}K)[b]	0.0330 ± 0.0043 [Le08]		0.0330 ± 0.0043	
		gs			$\mathbf{99.9670^{+0.0043}_{-0.0044}}$	
^{42}Sc	^{42}Ca	1.84	0.0063 ± 0.0026 [In77]	0.0022 ± 0.0017 [De78]		
			0.0103 ± 0.0031 [Sa80]	0.0070 ± 0.0012 [Da85]	0.0059 ± 0.0014	1.6
		gs			**99.9941 ± 0.0014**	
^{46}V	^{46}Ti	2.61	0.0039 ± 0.0004 [Ha94]		0.0039 ± 0.0004	
		4.32	0.0113 ± 0.0012 [Ha94]		0.0113 ± 0.0012	
		ΣGT[c]	<0.01		$0.00^{+0.01}_{-0}$	
		gs			$\mathbf{99.9848^{+0.0013}_{-0.0042}}$	
^{50}Mn	^{50}Cr	3.63	0.057 ± 0.003 [Ha94]		0.057 ± 0.003	
		3.85	<0.0003 [Ha94]		$0.0000^{+0.0003}_{-0}$	
		5.00	0.0007 ± 0.0001 [Ha94]		0.0007 ± 0.0001	
		gs			**99.9423 ± 0.0030**	
^{54}Co	^{54}Fe	2.56	0.0045 ± 0.0006 [Ha94]		0.0045 ± 0.0006	
		ΣGT[c]	<0.03		$0.00^{+0.03}_{-0}$	
		gs			$\mathbf{99.9955^{+0.0006}_{-0.0300}}$	
^{62}Ga	^{62}Zn	ΣGT[c]	0.142 ± 0.008 [Fi08]	0.107 ± 0.024 [Be08]	0.139 ± 0.011	1.4
		gs			**99.862 ± 0.011**	
^{74}Rb	^{74}Kr	ΣGT[c]	0.5 ± 0.1 [Pi03]	0.455 ± 0.031 [Du13]	0.459 ± 0.030	
		gs			**99.541 ± 0.030**	

[a]Result also incorporates data from Table V.

[b]The decay of ^{38m}K includes a weak γ-ray branch to the ^{38}K ground state, which competes with the β decay.

[c]Designates total Gamow-Teller transitions to levels not explicitly listed; in cases where upper limits are shown, they were derived with the help of calculations in [Ha02] or with refined versions of those calculations.

traps are clearly capable of measuring the mass of trapped ions to much higher accuracy than that, but it is not easy to identify the nuclear state they are measuring. It is likely in this case that the trap actually measured an isomeric state in ^{70}Br rather than its ground state. Of course, arguments based on systematics are not infallible either and, in any case, this Q_{EC} value needs to be determined more precisely. Fresh experiments are certainly called for.

TABLE V. Relative intensities of β-delayed γ rays in the superallowed β-decay daughters. These data are used to determine some of the branching ratios presented in Table IV. (See Table VIII for the correlation between the alphabetical reference code used in this table and the actual reference numbers.)

Parent/daughter nuclei		Daughter ratios[a]	Measured γ-ray ratio		Average value	
			1	2	Ratio	Scale
^{18}Ne	^{18}F	$\gamma_{660}/\gamma_{1042}$	0.0169 ± 0.0004 [He82]	0.0172 ± 0.0005 [Ad83]		
			0.01733 ± 0.00012 [Gr13]		0.01729 ± 0.00011	1.0
^{26}Si	^{26}Al	$\gamma_{1622}/\gamma_{829}$	0.149 ± 0.016 [Mo71]	0.134 ± 0.005 [Ha75]		
			0.1245 ± 0.0023 [Wi80]	0.1301 ± 0.0062 [Ma08]	0.1269 ± 0.0026	1.3
		$\gamma_{1655}/\gamma_{829}$	0.00145 ± 0.00032 [Wi80]		0.00145 ± 0.00032	
		$\gamma_{1843}/\gamma_{829}$	0.013 ± 0.003 [Mo71]	0.016 ± 0.003 [Ha75]		
			0.01179 ± 0.00027 [Wi80]		0.01183 ± 0.00027	1.0
		$\gamma_{2512}/\gamma_{829}$	0.00282 ± 0.00010 [Wi80]		0.00282 ± 0.00010	
		$\gamma_{\text{total}}/\gamma_{829}$			0.1430 ± 0.0026	
^{30}S	^{30}P	$\gamma_{709}/\gamma_{677}$	0.006 ± 0.003 [Mo71]	0.0037 ± 0.0009 [Wi80]	0.0039 ± 0.0009	1.0
		$\gamma_{2341}/\gamma_{677}$	0.033 ± 0.002 [Mo71]	0.0290 ± 0.0006 [Wi80]	0.0293 ± 0.0011	1.9
		$\gamma_{3019}/\gamma_{677}$	0.00013 ± 0.00006 [Wi80]		0.00013 ± 0.00006	
		$\gamma_{\text{total}}/\gamma_{677}$			0.0334 ± 0.0014	
^{34}Ar	^{34}S	$\gamma_{461}/\gamma_{666}$	0.28 ± 0.16 [Mo71]	0.365 ± 0.036 [Ha74a]	0.361 ± 0.035	1.0
		$\gamma_{2580}/\gamma_{666}$	0.38 ± 0.09 [Mo71]	0.345 ± 0.010 [Ha74a]	0.345 ± 0.010	1.0
		$\gamma_{3129}/\gamma_{666}$	0.67 ± 0.08 [Mo71]	0.521 ± 0.012 [Ha74a]	0.524 ± 0.022	1.8
		$\gamma_{\text{total}}/\gamma_{666}$			1.231 ± 0.043	
^{42}Ti	^{42}Sc	$\gamma_{2223}/\gamma_{611}$	0.012 ± 0.004 [Ga69]		0.012 ± 0.004	
		$\gamma_{\text{total}}/\gamma_{611}$	0.023 ± 0.012 [Ga69,En90]		0.023 ± 0.012	

[a] γ-ray intensities are denoted by γ_E, where E is the γ-ray energy in keV.

The half-life data appear in Table III in similar format to Table I. For obvious reasons, half-life measurements do not lend themselves to being updated. Consequently, a number of mostly pre-1970 measurements have been rejected because they were not analyzed with the "maximum-likelihood" method. The importance of using this technique for precision measurements was not recognized until 1969 [71] and, without access to the primary data, there is no way a new analysis can

TABLE VI. References for which the original decay-energy results have been updated to incorporate the most recent calibration standards. (See Table VIII for the correlation between the alphabetical reference code used in this table and the actual reference numbers.)

References (parent nucleus)[a]	Update procedure
Bo64 (^{18}Ne), Ba84 (^{10}C), Br94 (^{26m}Al) Ba98 (^{10}C), Ha98 (^{38m}K), To03 (^{14}O)	We have converted all original (p,n) threshold measurements to Q values using the most recent mass excesses [Wa12].
Wh77 (^{14}O)	This (p,n) threshold measurement has been adjusted to reflect more recent calibration α energies [Ry91] before being converted to a Q value.
Pr67 (^{18}Ne)	Before conversion to a Q value, this (p,n) threshold was adjusted to reflect a new value for the ^{7}Li(p,n) threshold [Wh85], which was used as calibration.
Bu61 (^{14}O), Ba62 (^{14}O)	These ^{12}C(^{3}He, n) threshold measurements have been adjusted for updated calibration reactions based on current mass excesses [Wa12].
Ha74d (^{34}Cl)	This (^{3}He, t) reaction Q value was calibrated by the ^{27}Al(^{3}He, t) reaction to excited states in ^{27}Si; it has been revised according to modern mass excesses [Wa12] and excited-state energies [En98].
Ba88 and Ba89 (^{10}C)	These measurements of excitation energies in ^{10}B have been updated to modern γ-ray standards [He00].
Ki89 (^{42}Sc)	This ^{41}Ca(p,γ) reaction Q value was measured relative to that for ^{40}Ca(p,γ); we have slightly revised the result based on modern mass excesses [Wa12].
Ha74c (^{22}Mg, ^{26}Si, ^{30}S, ^{34}Ar)	These (p,t) reaction Q values have been adjusted to reflect the current Q value for the ^{16}O(p,t) reaction [Wa12], against which they were calibrated.

[a] These references all appear in Table I under the appropriate parent nucleus.

TABLE VII. References from which some or all results have been rejected even though their quoted uncertainties qualified them for inclusion. (See Table VIII for the correlation between the alphabetical reference code used in this table and the actual reference numbers.)

References (parent nucleus)	Reason for rejection
1. Decay energies	
Pa72 (^{30}S)	No calibration is given for the measured (p,t) reaction Q values; update is clearly required but none is possible.
No74 (^{22}Mg)	Calibration reaction Q values have changed but calibration process is too complex to update.
Ro74 (^{10}C)	P. H. Barker (coauthor) later considered that inadequate attention had been paid to target surface purity [Ba84].
Ba77b (^{10}C)	P. H. Barker (coauthor) later stated [Ba84] that the (p,t) reaction Q value could not be updated to incorporate modern calibration standards.
Vo77 (^{14}O, ^{26}Al^{m}, ^{34}Cl, ^{42}Sc, ^{46}V, ^{50}Mn, ^{54}Co)	Most of the results in this reference disagree significantly with more recent and accurate measurements. A detailed justification for rejection is presented in our 2009 survey [6].
Wh81 and Ba98 (^{14}O)	The result in [Wh81] was updated in [Ba98] but then eventually withdrawn by P. H. Barker (coauthor) in [To03].
Sa09 (^{70}Br)	The result is inconsistent with Q_{EC}-value systematics. See text (Sec. II B).
2. Half-lives	
He61 (^{14}O), Ba62 (^{14}O), Fr63 (^{14}O), Fr65 (^{42}Sc, ^{50}Mn), Si72 (^{14}O)	Quoted uncertainties are too small, and results likely biased, in light of statistical difficulties more recently understood (see [Fr69a]). In particular, "maximum-likelihood" analysis was not used.
Ha72a (^{34}Cl, ^{42}Sc)	All four quoted half-lives are systematically higher than more recent and accurate measurements.
Ro74 (^{10}C)	P. H. Barker (coauthor) later considered that pile-up had been inadequately accounted for [Ba90].
Ch84 (^{38m}K)	"Maximum-likelihood" analysis was not used.
Ma08 (^{26}Si)	No account was taken of the β-detection-efficiency difference between the parent and daughter activities. See [Ia10] for a more detailed explanation.
3. Branching ratios	
Fr63 (^{26}Si)	Numerous impurities present; result is obviously wrong.

be applied retroactively. All rejected half-life measurements are also documented in Table VII.

Finally, the branching-ratio measurements are presented in Table IV. The decays of the $T_z = 0$ parents are the most straightforward because, in all these cases, the superallowed branch accounts for >99.5% of the total decay strength. Thus, even imprecise measurements of the weak nonsuperallowed branches can be subtracted from 100% to yield the superallowed branching ratio with good relative precision. For the higher-Z parents of this type, particularly ^{62}Ga and heavier, it has been shown theoretically [93] and experimentally ([66] for ^{62}Ga, and [55,142] for ^{74}Rb) that numerous very-weak Gamow-Teller transitions occur, which, in total, can carry significant decay strength. Where such unobserved transitions are expected to exist but have not already been accounted for in the quoted references, we have used a combination of experiment and theory to arrive at an upper limit for the unobserved strength, with uncertainties being adjusted accordingly.

The branching ratios for decays from $T_z = -1$ parents are much more challenging to determine, because the superallowed branch is usually one of several strong branches—with the notable exception of ^{14}O—and, in two of the measured cases, it actually has a branching ratio of less than 10%. For the decays of ^{22}Mg and ^{38}Ca, the superallowed branching ratio has been experimentally determined and the result published, so no special treatment was required for them. However, the decays of ^{18}Ne, ^{26}Si, ^{30}S, ^{34}Ar, and ^{42}Ti had to be treated differently. In each case, the absolute branching ratio for a single β transition has been measured. The branching ratios for other β transitions then had to be determined from the relative intensities of β-delayed γ rays in the daughter. The relevant γ-ray intensity measurements appear in Table V, with their averages then being used to determine the superallowed branching-ratio averages shown in bold type in Table IV. These cases are also flagged with a footnote in that table.

TABLE VIII. Reference key, relating alphabetical reference codes used in Tables I–VII to the actual reference numbers.

Table code	Reference No.	Table code	Reference No.	Table code	Reference No.	Table code	Reference No.	Table code	Reference No.	Table code	Reference No.
Ad83	[7]	Aj88	[8]	Aj91	[9]	Al69	[10]	Al72	[11]	Al75	[12]
Al77	[13]	Al78	[14]	Al82	[15]	An70	[16]	Az74	[17]	Az75	[18]
Ba62	[19]	Ba77a	[20]	Ba77b	[21]	Ba84	[22]	Ba88	[23]	Ba89	[24]
Ba90	[25]	Ba98	[26]	Ba00	[27]	Ba01	[28]	Ba04	[29]	Ba06	[30]
Ba09	[31]	Ba10	[32]	Be68	[33]	Be78	[34]	Be85	[35]	Be08	[36]
Bi03	[37]	Bl04a	[38]	Bl04b	[39]	Bl10	[40]	Bo64	[41]	Br94	[42]
Bu61	[43]	Bu88	[44]	Bu06	[45]	Ca05	[46]	Ch84	[47]	Ch13	[48]
Cl73	[49]	Da80	[50]	Da85	[51]	De69	[52]	De78	[53]	Dr75	[54]
Du13	[55]	En90	[56]	En98	[57]	Er06a	[58]	Er06b	[59]	Er08	[60]
Er09a	[61]	Er09b	[62]	Er11	[63]	Et11	[64]	Fa09	[65]	Fi08	[66]
Fi11	[67]	Fi12	[68]	Fr63	[69]	Fr65	[70]	Fr69a	[71]	Fr75	[72]
Fu99	[73]	Ga69	[74]	Ga01	[75]	Ge07	[76]	Ge08	[77]	Gi72	[78]
Go72	[79]	Gr07	[80]	Gr08	[81]	Gr13	[82]	Ha67	[83]	Ha68	[84]
Ha72a	[85]	Ha74a	[86]	Ha74b	[87]	Ha74c	[88]	Ha74d	[89]	Ha75	[90]
Ha94	[91]	Ha98	[92]	Ha02	[93]	Ha03	[94]	He61	[95]	He81	[96]
He82	[97]	He00	[98]	He01	[99]	He02	[100]	Ho64	[101]	Ho74	[102]
Hu82	[103]	Hy03	[104]	Hy05	[105]	Ia06	[106]	Ia08	[107]	Ia10	[108]
In77	[109]	Is80	[110]	Je07	[111]	Ji02	[112]	Ka69	[113]	Ke07	[114]
Ki89	[115]	Ki91	[116]	Ko83	[117]	Ko87	[118]	Ko97a	[119]	Ko97b	[120]
Kr91	[121]	Ku09	[122]	Kw10	[123]	Kw13	[124]	La13	[125]	Le08	[126]
Li94	[127]	Ma94	[128]	Ma08	[129]	Mc67	[130]	Mi67	[131]	Mo71	[132]
Mu04	[133]	Na91	[134]	No74	[135]	Oi01	[136]	Pa72	[137]	Pa05	[138]
Pa11	[139]	Pa12	[140]	Pa14	[141]	Pi03	[142]	Pr67	[143]	Pr90	[144]
Ra83	[145]	Re85	[146]	Ri07	[147]	Ro70	[148]	Ro72	[149]	Ro74	[150]
Ro75	[151]	Ro06	[152]	Ry73	[153]	Ry91	[154]	Sa80	[155]	Sa95	[156]
Sa04	[157]	Sa05	[158]	Sa09	[159]	Sc07	[160]	Sc11	[161]	Se73	[162]
Se05	[163]	Sh55	[164]	Si66	[165]	Si72	[166]	So11	[167]	Sq75	[168]
Ta12	[169]	Ti95	[170]	To03	[171]	To05	[172]	Vo77	[173]	Wa83	[174]
Wa92	[175]	Wa12	[176]	We68	[177]	Wh77	[178]	Wh81	[179]	Wh85	[180]
Wi76	[181]	Wi78	[182]	Wi80	[183]	Zi87	[184]				

III. THE $\mathcal{F}t$ VALUES

With the input data now settled, we can proceed to derive the ft values for the 20 superallowed transitions included in the tables. We calculate the statistical rate function f using the same code as in our previous survey. The basic methodology for the calculation is described in the Appendix to our 2004 survey [5], with refinements applied to incorporate excitation of the daughter atom, as explained in Appendix A of our 2008 survey [6]. Our final f values for the $T = 1$ transitions of interest here are recorded in the second column of Table IX. They were evaluated with the $Q_{\rm EC}$ values and their uncertainties taken from column 7 of Table I.

The third column of Table IX lists (as percentages) the electron-capture fraction, $P_{\rm EC}$, calculated for each of the 20 superallowed transitions. The method of calculation was described in our 2004 survey [5], to which the reader is referred for more details. The partial half-life, t, for each transition is then obtained from its total half-life, $t_{1/2}$, branching ratio, R, and electron-capture fraction according to the following formula:

$$t = \frac{t_{1/2}}{R}\,(1 + P_{\rm EC})\,. \qquad (2)$$

The resultant values for the partial half-lives and the corresponding ft values appear in columns 4 and 5 of the table.

To obtain the $\mathcal{F}t$ from each ft value, we use Eq. (1) to apply the small transition-dependent correction terms, δ'_R, $\delta_{\rm NS}$ and δ_C. The values we use for δ'_R appear in column 6 of Table IX while those of δ_C-$\delta_{\rm NS}$, the combination of the other two terms that appears in Eq. (1), are given in column 7. Finally, column 8 of the table contains the derived $\mathcal{F}t$ values and, at the bottom of the column, their average, $\overline{\mathcal{F}t}$. The three theoretical corrections applied here, together with the transition-independent radiative correction $\Delta_{\rm R}^{\rm V}$, which is ultimately needed to extract V_{ud}, is described in more detail in the following section.

A. Theoretical corrections

Of the four theoretical correction terms—$\Delta_{\rm R}^{\rm V}$, δ'_R, $\delta_{\rm NS}$, and δ_C—that appear in Eq. (1) the first three are radiative corrections, and the fourth is the isospin-symmetry-breaking correction. In the following two sections, one for each category of correction, we briefly describe all four correction terms and give the sources and justification of the values we use for them.

TABLE IX. Derived results for superallowed Fermi β decays.

Parent nucleus	f	P_{EC} (%)	Partial half-life t (ms)	ft (s)	δ'_R (%)	$\delta_C - \delta_{NS}$ (%)	$\mathcal{F}t$ (s)
$T_z = -1$							
^{10}C	2.30169 ± 0.00070	0.299	1322100 ± 1800	3043.0 ± 4.3	1.679	0.520 ± 0.039	3078.0 ± 4.5[a]
^{14}O	42.771 ± 0.023	0.088	71126 ± 50	3042.2 ± 2.7	1.543	0.575 ± 0.056	3071.4 ± 3.2[a]
^{18}Ne	134.64 ± 0.17	0.081	21640 ± 590	2914 ± 79	1.506	0.850 ± 0.052	2932.8 ± 80
^{22}Mg	418.37 ± 0.17	0.069	7295 ± 17	3051.9 ± 7.2	1.466	0.605 ± 0.030	3077.9 ± 7.3[a]
^{26}Si	1028.03 ± 0.12	0.064	2976 ± 23	3059 ± 23	1.438	0.650 ± 0.034	3083 ± 23
^{30}S	1976.71 ± 0.56	0.066	1520 ± 21	3005 ± 41	1.423	1.040 ± 0.032	3016 ± 41
^{34}Ar	3410.97 ± 0.61	0.069	894.0 ± 2.4	3049.6 ± 8.1	1.412	0.875 ± 0.058	3065.6 ± 8.4[a]
^{38}Ca	5328.88 ± 0.30	0.075	574.7 ± 1.3	3062.3 ± 6.8	1.414	0.940 ± 0.072	3076.4 ± 7.2[a]
^{42}Ti	7130.5 ± 1.4	0.087	437 ± 12	3114 ± 84	1.428	1.175 ± 0.080	3121 ± 84
$T_z = 0$							
^{26m}Al	478.232 ± 0.081	0.083	$6351.26^{+0.54}_{-0.55}$	3037.38 ± 0.58	1.478	0.305 ± 0.027	3072.9 ± 1.0[a]
^{34}Cl	1996.003 ± 0.096	0.080	$1527.77^{+0.44}_{-0.47}$	$3049.43^{+0.88}_{-0.95}$	1.443	0.735 ± 0.048	$3070.7^{+1.7}_{-1.8}$[a]
^{38m}K	3297.39 ± 0.15	0.085	925.42 ± 0.28	3051.45 ± 0.92	1.440	0.770 ± 0.056	3071.6 ± 2.0[a]
^{42}Sc	4472.23 ± 1.15	0.099	681.44 ± 0.26	3047.5 ± 1.4	1.453	0.630 ± 0.059	3072.4 ± 2.3[a]
^{46}V	7209.25 ± 0.54	0.101	$423.113^{+0.053}_{-0.068}$	$3050.32^{+0.44}_{-0.46}$	1.445	0.655 ± 0.063	3074.1 ± 2.0[a]
^{50}Mn	$10\,745.97 \pm 0.50$	0.107	283.68 ± 0.11	3048.4 ± 1.2	1.444	0.685 ± 0.055	3071.2 ± 2.1[a]
^{54}Co	$15\,766.7 \pm 2.9$	0.111	$193.493^{+0.063}_{-0.086}$	$3050.7^{+1.1}_{-1.5}$	1.443	0.805 ± 0.068	$3069.8^{+2.4}_{-2.6}$[a]
^{62}Ga	$26\,400.3 \pm 8.3$	0.135	116.440 ± 0.042	3074.0 ± 1.5	1.459	1.52 ± 0.21	3071.5 ± 6.7[a]
^{66}As	$32\,120 \pm 460$	0.153			1.468	1.61 ± 0.40	
^{70}Br	$38\,600 \pm 3600$	0.173			1.49	1.78 ± 0.25	
^{74}Rb	47281 ± 93	0.191	65.199 ± 0.047	3082.7 ± 6.5	1.50	1.69 ± 0.27	3076 ± 11[a]
						Average (best 14), $\overline{\mathcal{F}t}$	3072.27 ± 0.62
						χ^2/ν	0.52

[a]Values used to obtain $\overline{\mathcal{F}t}$.

1. *Radiative corrections*

In a β-decay half-life experiment, the rate measured includes not only the bare-decay but also radiative-decay processes, such as bremsstrahlung. Since it is the half-life of the bare β-decay process that is required for the ft value, the measured result has to be amended with a radiative-correction calculation. The principal graphs to be evaluated are the one-photon bremsstrahlung, the γW-box, and ZW-box diagrams. For calculational convenience it is standard to separate the contributions from these graphs into contributions at high photon energies (short distances) and low photon energies (long distances).

The short-distance correction includes the ZW-box and the high-energy part of the γW-box diagrams and is evaluated by ignoring the hadronic structure and using free-quark Lagrangians. This contribution therefore is universal, being independent of which particular nucleus is involved in the β decay. We denote this contribution Δ_R^V and, it being universal, we place it on the right-hand side of Eq. (1). The current best value, which we adopt from Marciano and Sirlin [186], is

$$\Delta_R^V = (2.361 \pm 0.038)\%. \quad (3)$$

The long-distance correction includes the bremsstrahlung and the low-energy part of the γW-box diagram; it requires a model calculation of the hadronic structure. Contributions to this correction have been calculated [187–191] to order α, α^2, and $Z\alpha^2$, and estimated from the leading-log term in order $Z^2\alpha^3$, where α is the fine-structure constant. In the latter two orders, the positron in the γW-box and bremsstrahlung diagrams interacts with the Coulomb field of the nucleus. We have listed the contributions from each order in Table V of Ref. [192] so here we only show their sums, δ'_R, for all the transitions of interest. These appear in column 2 of Table X, the table which collects all the theoretical correction terms, and also, for convenience, in column 6 of Table IX, which collects all the input to the left-hand side of Eq. (1).

In contrast with our previous surveys, we list no uncertainties on the individual δ'_R values. In the past, we have taken the uncertainty on each transition's δ'_R value to be equal to the entire $Z^2\alpha^3$ contribution. We have then treated the uncertainty as being statistical, adding it in quadrature to the experimental uncertainty to obtain the total uncertainty on the $\mathcal{F}t$ value for that transition. The latter was, in turn, handled statistically in the derivation of an average $\overline{\mathcal{F}t}$ for all the transitions.

We have now revised this prescription in two ways. First, we reduce the magnitude of the uncertainty on δ'_R to one-third of the $Z^2\alpha^3$ term, and second, we treat it as a systematic, rather than a statistical effect. Our previous choice for the magnitude originated 25 years ago with Sirlin [188], who at the time did not include the $Z^2\alpha^3$ term in the radiative correction itself but used it only as an estimate of its uncertainty. One year later, though, he chose instead to include it in the correction itself [190], while apparently neglecting any contribution to the uncertainty. We now believe that our choice to combine both these approaches by including the $Z^2\alpha^3$ term in δ'_R and also assigning it to be the latter's uncertainty was being overly

TABLE X. Corrections δ'_R, δ_{NS}, and δ_C that are applied to experimental ft values to obtain $\mathcal{F}t$ values.

Parent nucleus	δ'_R (%)	δ_{NS} (%)	δ_{C1} (%)	δ_{C2} (%)	δ_C (%)
$T_z = -1$					
^{10}C	1.679	−0.345(35)	0.010(10)	0.165(15)	0.175(18)
^{14}O	1.543	−0.245(50)	0.055(20)	0.275(15)	0.330(25)
^{18}Ne	1.506	−0.290(35)	0.155(30)	0.405(25)	0.560(39)
^{22}Mg	1.466	−0.225(20)	0.010(10)	0.370(20)	0.380(22)
^{26}Si	1.439	−0.215(20)	0.030(10)	0.405(25)	0.435(27)
^{30}S	1.423	−0.185(15)	0.155(20)	0.700(20)	0.855(28)
^{34}Ar	1.412	−0.180(15)	0.030(10)	0.665(55)	0.695(56)
^{38}Ca	1.414	−0.175(15)	0.020(10)	0.745(70)	0.765(71)
^{42}Ti	1.427	−0.235(20)	0.105(20)	0.835(75)	0.940(78)
$T_z = 0$					
^{26m}Al	1.478	0.005(20)	0.030(10)	0.280(15)	0.310(18)
^{34}Cl	1.443	−0.085(15)	0.100(10)	0.550(45)	0.650(46)
^{38m}K	1.440	−0.100(15)	0.105(20)	0.565(50)	0.670(54)
^{42}Sc	1.453	0.035(20)	0.020(10)	0.645(55)	0.665(56)
^{46}V	1.445	−0.035(10)	0.075(30)	0.545(55)	0.620(63)
^{50}Mn	1.444	−0.040(10)	0.035(20)	0.610(50)	0.645(54)
^{54}Co	1.443	−0.035(10)	0.050(30)	0.720(60)	0.770(67)
^{62}Ga	1.459	−0.045(20)	0.275(55)	1.20(20)	1.48(21)
^{66}As	1.468	−0.060(20)	0.195(45)	1.35(40)	1.55(40)
^{70}Br	1.486	−0.085(25)	0.445(40)	1.25(25)	1.70(25)
^{74}Rb	1.499	−0.075(30)	0.115(60)	1.50(26)	1.62(27)

cautious. Furthermore, because the uncertainty is associated with the $Z^2\alpha^3$ term, it is expected to be a smooth function of Z^2 and thus to behave systematically since any shift in the value of δ'_R must affect all $\mathcal{F}t$ values in the same direction.

We then proceed as follows: We evaluate the individual transition $\mathcal{F}t$ values without including any uncertainties associated with δ'_R and obtain an average $\overline{\mathcal{F}t}$. Then we shift all the individual δ'_R terms up and down by one-third of the $Z^2\alpha^3$ contribution, recalculate the $\mathcal{F}t$ values and determine $\overline{\mathcal{F}t}$ for both. The shifts in the value of the latter—± 0.36 s for the data in Table IX—becomes the systematic uncertainty assigned to $\overline{\mathcal{F}t}$ to account for the uncertainty in δ'_R. Note that our choice to take one-third of the $Z^2\alpha^3$ term is rather arbitrary, but has the benefit that it is still conservative and at the same time results in the uncertainty in δ'_R having an impact on the overall result that is comparable to its impact in our previous survey [6].

We turn now to the third radiative term δ_{NS}, which arises from an evaluation of the low-energy part of the γW-box graph for an axial-vector weak interaction. If it is assumed that the γN and WN vertices are both with the same nucleon, N, then the evaluated box graph becomes proportional to the Fermi β-decay operator, yielding a universal correction already included in Δ_R^V.

If instead the γ and W interactions in the γW-box graph for an axial-vector current are with different nucleons in the nucleus, then the evaluation involves two-nucleon operators, which necessitates a nuclear-structure calculation. This component of the radiative correction we denote by δ_{NS} and list its values in column 3 of Table X. The values and their uncertainties have been taken from Table VI in Ref. [192]. For this correction term, a number of model calculations were carried out for each nucleus [192] and the uncertainties listed were chosen to encompass the spread in the results from these calculations. Therefore the uncertainty is nucleus-specific and, as such, can be treated as statistical and not systematic. We thus combine it in quadrature with the experimental errors in determining the $\mathcal{F}t$-value uncertainties.

2. *Isospin-symmetry-breaking correction*

In this section we describe only the set of isospin-symmetry-breaking corrections, δ_C, that we have used in deriving the corrected $\mathcal{F}t$ values given in Table IX. A discussion of other alternative calculations of δ_C—and our reasons for rejecting them—is postponed to Sec. IV. The set we have selected follows from a semiphenomenological approach based on the shell model combined with Woods-Saxon radial functions. This model, which we designate as SM-WS, has been described in detail by us in Ref. [192], where also the results for δ_C are tabulated. We describe the model only briefly here, while making two minor updates to our previous results.

The calculation is done in two parts, which is made possible by our dividing δ_C into two terms:

$$\delta_C = \delta_{C1} + \delta_{C2}. \tag{4}$$

The idea is that δ_{C1} follows from a tractable shell-model calculation that does not include significant nodal mixing, while δ_{C2} corrects for the nodal mixing that would be present if the shell-model space were much larger.

For δ_{C1}, a modest shell-model space (usually one major oscillator shell) is employed, in which Coulomb and other charge-dependent terms are added to the charge-independent effective Hamiltonian customarily used for the shell model. These charge-dependent additional terms are separately adjusted for each superallowed β transition to reproduce the b and c coefficients of the isobaric multiplet mass equation (IMME) for the triplet of $T = 1$, 0^+ states that includes the parent and daughter states of the transition.

Since the Coulomb force is long range, its influence in configuration space extends much further than the single major oscillator shell included in the calculation of δ_{C1}. To incorporate the effects of multishell mixing, we note first that its principal impact is to change the structure of the radial wave function by introducing mixing with radial functions that have more nodes. Since this mixing primarily affects protons, it results in proton radial functions that differ from the neutron ones so, when the overlap is computed, its departure from unity determines the value of δ_{C2}. The radial functions themselves are derived from a Woods-Saxon potential. Again there is a case-by-case adjustment in the Woods-Saxon potentials to ensure that the different measured proton and neutron separation energies in the β-decay parents and daughters are correctly reproduced.

The SM-WS calculations of Towner and Hardy [192] must clearly be classified as semiphenomenological. A number of transition-specific nuclear properties have been fitted in their determination of δ_C. In contrast, most of the alternative models discussed in Sec. IV are first-principles theory calculations.

They have no local phenomenological constraints and therefore are not capable of offering the precision required for our $\mathcal{F}t$ analysis. Nevertheless, they play a very important role in confirming that the semiphenomenological results are not inconsistent with the broad features predicted by a first-principles calculation.

The values we use for δ_{C1} are given in column 4 of Table X. They differ slightly from the published values in [192] because a new compilation of IMME coefficients by MacCormick and Audi [193], based on the 2012 atomic mass evaluation [194], has made small changes to these coefficients. Also, there are still insufficient experimental data for nuclei in the upper pf shell, so the compilation of coefficients for $T = 1$ multiplets ends at $A = 58$. For the four superallowed decays from ^{62}Ga to ^{74}Rb, we have used an extrapolation formula [193] to estimate the c coefficients and then used the relation $Q_{\rm EC} = -b - c$ to obtain the b coefficient for each case. With these new IMME coefficients, we reevaluated all the δ_{C1} values, yielding the results shown in Table X.

The values we use for δ_{C2} are shown in column 5 of Table X and are the same as those previously published [192] for all but four cases where an update has been effected. To explain the origin of the update we need to explain some details of the δ_{C2} calculation: As already mentioned, the radial functions used to calculate the radial overlap are taken to be eigenfunctions of a phenomenological Woods-Saxon potential. The radius parameter of this potential is determined by our requiring that the charge density constructed from the proton eigenfunctions of the potential yields a root-mean-charge radius in agreement with the experimental value measured by electron scattering [195]. However, in most cases the experimental charge radius is known only for the stable isotope of the element of interest, whereas our need is for the radius of the unstable β-decaying isotope. Thus, we add an estimated isotope shift to the nearby measured rms radius and apply a generous uncertainty. This uncertainty is only one of three contributions to the final uncertainty quoted for each δ_{C2} value. The other two account for (a) the scatter in the results from three different methodologies and (b) the scatter in the results from different shell-model interactions used to compute the required spectroscopic amplitudes [196].

The issue of the appropriate experimental charge radius has not been revisited since our 2002 work [196]. Since then, a new compilation of charge radii has been published [197], including not only results from electron scattering, but also values obtained from muonic-atom x rays, K_α isotope shifts, and optical shifts. In this compilation, radii are given for three of the β-decaying isotopes of relevance to our superallowed β-decay studies: ^{18}Ne, ^{34}Ar, and ^{38m}K. In addition, more recently, collinear-laser spectroscopy on the neutron-deficient Rb isotopes enabled the charge radius of ^{74}Rb to be determined from its hyperfine splitting [198]. For these four cases, therefore, we have recomputed the δ_{C2} correction.

For the lightest three cases, ^{18}Ne, ^{34}Ar, and ^{38m}K, the change in the rms charge radius was sufficient to produce a noticeable shift in the δ_{C2} value, though not outside our previously quoted uncertainty. Unfortunately, though, the reduction in the error on the rms charge radius did not significantly lower the overall uncertainty assigned to δ_{C2} because in all three cases the uncertainty is dominated by the spread in the results obtained from the three different methodologies. For the heaviest case, ^{74}Rb, the revision in the rms radius was small, so it made no change in the value of δ_{C2} but did reduce its uncertainty. However, even though the uncertainty in the radius was reduced by a factor of ten, it only led to a 20% reduction in the uncertainty for δ_{C2}. For all four cases the revised results appear in Table X.

The sum of δ_{C1} and δ_{C2} is shown in the last column of Table X. As with $\delta_{\rm NS}$, uncertainties have been assigned to δ_C which are nucleus specific. They represent the spread of results obtained with different shell-model interactions and different methodologies, as well as uncertainties in rms radii and IMME coefficients: all for the specific nuclei involved in each transition. We therefore treat them subsequently as statistical uncertainties.

B. Consistency of $\mathcal{F}t$ values

The experimental and theoretical results appearing in columns 2–7 of Table IX have been treated as input to Eqs. (1) and (2), from which we derive the $\mathcal{F}t$ values listed in column 8. All the input uncertainties that appear in the table are combined in quadrature to obtain the $\mathcal{F}t$-value uncertainties.

There are now 14 superallowed transitions whose $\mathcal{F}t$ values have uncertainties less than $\pm 0.4\%$, with the best case, ^{26}Al^m, being known an order of magnitude better than that. The uncorrected ft values and the fully corrected $\mathcal{F}t$ values for these transitions are plotted as a function of the daughter Z values in the top and bottom panels, respectively, of Fig. 2. Readily evident is the remarkable efficacy of the applied corrections in converting the scatter of the ft values into a self-consistent set of $\mathcal{F}t$ values. Such consistency is an expectation of CVC and an essential prerequisite if the data are to be used in any further probes of the standard model. The results in column 8 of Table IX and the bottom panel of Fig. 2 clearly satisfy the test, the weighted average of the 14 most precise results being given at the bottom of column 8 along with the corresponding χ^2 per degree of freedom of $\chi^2/\nu = 0.52$.

Although the $\mathcal{F}t$-value results depend on theoretical correction terms in addition to primary experimental data, we treat all of the uncertainties in Table IX as being statistical in nature for reasons explained in Sec. III A. This leaves the uncertainty associated with δ'_R, which is derived as a systematic effect in Sec. III A 1, still to be applied to the average $\overline{\mathcal{F}t}$. Thus, the final result for $\overline{\mathcal{F}t}$ becomes

$$\begin{aligned}\overline{\mathcal{F}t} &= 3072.27 \pm 0.62_{\rm stat} \pm 0.36_{\delta'_R}\ {\rm s} \\ &= 3072.27 \pm 0.72\ {\rm s}, \end{aligned} \tag{5}$$

where the two uncertainties have been combined in quadrature on the second line. Since $\mathcal{F}t$ is inversely proportional to the *square* of the vector coupling constant, $G_{\rm V}$, then Eq. (5) can be said to confirm the constancy of $G_{\rm V}$—and to verify this key component of the CVC hypothesis—at the level of 1.2×10^{-4}.

Compared with the results of our last survey [6], the value of $\overline{\mathcal{F}t}$ in Eq. (5) is somewhat higher, though well within the previous error bars, and carries a smaller uncertainty. The value

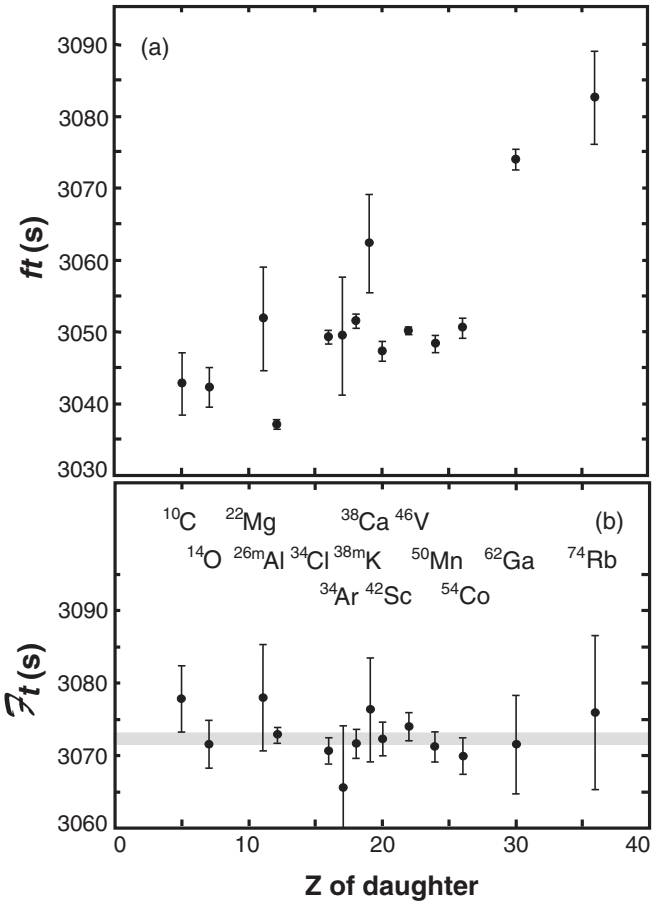

FIG. 2. (a) In the top panel are plotted the uncorrected experimental ft values as a function of the charge on the daughter nucleus. (b) In the bottom panel, the corresponding $\mathcal{F}t$ values are given; they differ from the ft values by the inclusion of the correction terms δ'_R, $\delta_{\rm NS}$, and δ_C. The horizontal gray band gives one standard deviation around the average $\overline{\mathcal{F}t}$ value.

of χ^2/ν associated with the current $\overline{\mathcal{F}t}$ result is higher than the corresponding value in 2008 but this undoubtedly reflects the fact that one additional transition has been added and the data for some of the other transitions are more precise today than they were 6 years ago. In any case, the confidence level for the new result remains very high: 91%.

C. Uncertainty budgets

We show the contributing factors to the individual $\mathcal{F}t$-value fractional uncertainties in two figures. The first, Fig. 3, encompasses the nine cases with stable daughter nuclei. Their experimental parameters have been measured with increasing precision for many years, so we refer to these as the "traditional nine." The remaining eleven cases, of which five now approach the traditional nine in precision, appear in Fig. 4. In both figures, the first three bars in each group of five show the contributions from experiment, while the last two correspond to theory. Although we are now treating the contribution from δ'_R as a systematic uncertainty that is applied to the final average $\overline{\mathcal{F}t}$, nevertheless we show a bar as a rough guide

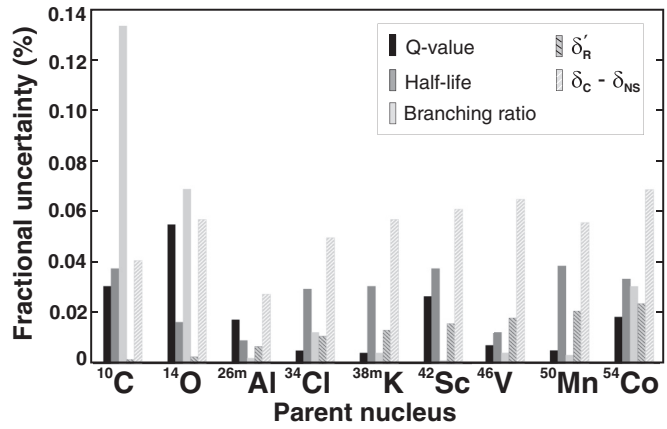

FIG. 3. Summary histogram of the fractional uncertainties attributable to each experimental and theoretical input factor that contributes to the final $\mathcal{F}t$ values for the "traditional nine" superallowed transitions. The bars for δ'_R are only a rough guide to the effect on each transition of this term's systematic uncertainty. See text.

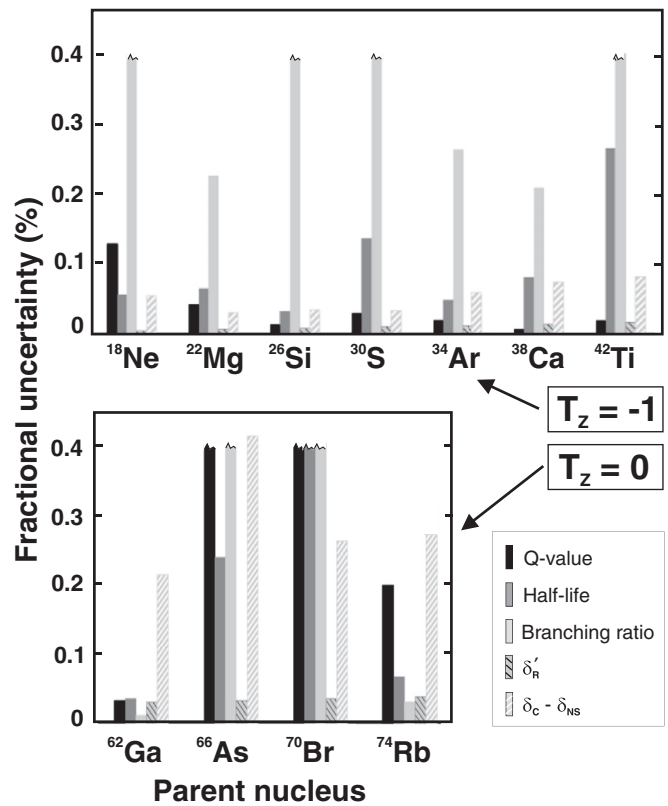

FIG. 4. Summary histogram of the fractional uncertainties attributable to each experimental and theoretical input factor that contributes to the final $\mathcal{F}t$ values for the 11 other superallowed transitions. Where the error is cut off with a jagged line at 40 parts in 10^4, no useful experimental measurement has been made. The bars for δ'_R are only a rough guide to the effect on each transition of this term's systematic uncertainty. See text.

to the significance of the δ'_R uncertainty for each transition. In each case, we take the height of that bar to correspond to one-third the size of the $Z^2\alpha^3$ term in the expression for δ'_R (see Sec. III A 1).

From Fig. 3, it can be seen that for seven of the nine transitions plotted there—all but those from ^{10}C and ^{14}O—the contributions from their three experimental uncertainties are substantially smaller than the corresponding contributions from the theoretical uncertainty due to the combined nuclear-structure-dependent corrections, $(\delta_C - \delta_{NS})$. The same can be said for the transitions from ^{62}Ga and ^{74}Rb, which appear among the $T_Z = 0$ cases illustrated in Fig. 4, although for these two cases the theoretical uncertainties are 3–10 times larger than they are for the lighter nuclei because of nuclear-model ambiguities.

There is good reason for these nine cases to have particularly small experimental uncertainties. They are all transitions from $T_Z = 0$ parent nuclei, which populate even-even daughters in which there are no, or very few, 1^+ states at low enough energy to be available for competing Gamow-Teller decays. Thus, the branching ratios for the superallowed transitions are all >99% and have very small associated uncertainties, the largest being for the decays of ^{54}Co and ^{74}Rb, which both have a 3×10^{-4} fractional uncertainty. In both cases, this is because they are predicted to have Gamow-Teller branches that are too weak to have been observed but numerous enough that their total strength is not negligible. To account for such competition, one must first make a sensitive search for weak branches and then resort to an estimate of the strength of the branches that could have been missed at the level of experimental sensitivity achieved. Such estimates are currently based on shell-model calculations, as first suggested in Ref. [93], and obviously they introduce some additional uncertainty.

The presence of numerous weak Gamow-Teller branches becomes an increasingly significant issue for the heavier-mass nuclei, which have increasingly large Q_{EC} values. For cases with $A \geqslant 62$, they present a major experimental challenge if they are to be fully characterized. To date this has been accomplished for the decays of ^{62}Ga [36,66] and ^{74}Rb [55] but at considerable effort. It remains to be seen if the same level of precision will ultimately be achievable for ^{66}As and ^{70}Br, the two other cases in the bottom panel of Fig. 4, or for the even heavier $T_Z = 0$ parents that extend beyond ^{74}Rb up to ^{98}In.

The decays of ^{10}C, ^{14}O, and all the transitions depicted in the top panel of Fig. 4 originate from $T_Z = -1$ parent nuclei and populate odd-odd daughters in which there are low-lying 1^+ states strongly fed by Gamow-Teller decay. These branches are of comparable intensity to the superallowed one so they—or the superallowed branch itself—must be measured directly with high relative precision, a very difficult proposition. The outcome is branching-ratio uncertainties that exceed all the other contributions to the $\mathcal{F}t$-value uncertainties, experimental or theoretical, for these cases. (Measurements of weak competing branches in the $T_Z = 0$ cases discussed in the previous paragraph require high sensitivity but not high relative precision because the total Gamow-Teller branching is more than a factor of 100 weaker than the superallowed branch for all of them.) Advances in experimental techniques for measuring branching ratios have improved the situation in recent years [94,141] and will improve it even more within the next few years. Nevertheless, it is unlikely that these cases will ever equal the overall level of precision already achieved for the $T_Z = 0$ parent decays. Their value lies instead in testing the calculated corrections for isospin-symmetry breaking [141], as described in Sec. IV C.

IV. ISOSPIN-SYMMETRY BREAKING

Our own isospin-symmetry-breaking calculations, which take a semiphenomenological approach based on the shell-model together with Woods-Saxon radial functions (denoted SM-WS), have been discussed in Sec. III A 2. The results obtained there for δ_C are listed in the last column of Table X and are repeated for comparison purposes in the second column of Table XI. Those are not the only calculations of δ_C. There are a number of others that have appeared in the literature, of which we outline some more recent entries here.

A. Other δ_C calculations

SM-HF. Ormand and Brown [199] were the first to suggest that the calculation of the radial overlap—i.e., the δ_{C2} component of δ_C—might be better served if a mean-field Hartree-Fock potential were used rather than the phenomenological Woods-Saxon potential. The most recent calculation of this type is by Hardy and Towner [6] and their results are listed

TABLE XI. Recent δ_C calculations (in percent units) based on models labeled SM-WS (shell-model, Woods-Saxon), SM-HF (shell-model, Hartree-Fock), RPA (random phase approximation), IVMR (isovector monopole resonance), and DFT (density functional theory). Also given is the χ^2/ν, χ^2 per degree of freedom, from the confidence test discussed in the text.

			RPA				
	SM-WS	SM-HF	PKO1	DD-ME2	PC-F1	IVMR[a]	DFT
$T_z = -1$							
^{10}C	0.175	0.225	0.082	0.150	0.109	0.147	0.650
^{14}O	0.330	0.310	0.114	0.197	0.150		0.303
^{22}Mg	0.380	0.260					0.301
^{34}Ar	0.695	0.540	0.268	0.376	0.379		
^{38}Ca	0.765	0.620	0.313	0.441	0.347		
$T_z = 0$							
^{26m}Al	0.310	0.440	0.139	0.198	0.159		0.370
^{34}Cl	0.650	0.695	0.234	0.307	0.316		
^{38m}K	0.670	0.745	0.278	0.371	0.294	0.434	
^{42}Sc	0.665	0.640	0.333	0.448	0.345		0.770
^{46}V	0.620	0.600					0.580
^{50}Mn	0.645	0.610					0.550
^{54}Co	0.770	0.685	0.319	0.393	0.339		0.638
^{62}Ga	1.475	1.205					0.882
^{74}Rb	1.615	1.405	1.088	1.258	0.668		1.770
χ^2/ν	1.4	6.4	4.9	3.7	6.1		4.3[b]

[a]Rodin [205] also computes $\delta_C = 0.992\%$ for both ^{66}As and ^{70}Br.
[b]The result for ^{62}Ga has not been included in the least-squares fit from which this value for χ^2/ν has been obtained.

in column 3 of Table XI. They considered the initial and final states for the β decay to be a core of $(A-1)$ nucleons, to which the last proton in the parent or the last neutron in the daughter is bound. They performed a spherical Skyrme-Hartree-Fock calculation for the $(A-1)$ nucleus with three different Skyrme interactions to obtain the mean fields for the binding potentials. One difficulty with this approach is that the Hartree-Fock procedure when carried out for a nucleus with $N \neq Z$ introduces spurious isospin mixing. No attempt was made to remove the spurious terms.

In a recent exploratory work, Le Bloas *et al.* [200] hope to get around this difficulty by performing the Hartree-Fock calculation in the even-even $N = Z$ nucleus with $A-2$ nucleons. The initial and final states for β decay are then constructed by adding a proton and a neutron to the Hartree-Fock core for the parent, and two neutrons for the daughter, while ensuring that the two additional particles are in time-reversal-invariant conjugate pairs. In preliminary calculations, they estimate a lower bound on the δ_C value to be of order 0.15% to 0.20%.

RPA. In this approach, a spherical Hartree-Fock calculation is performed on the even-even member of the pair of nuclei involved in a superallowed β-decay transition: the parent nucleus in the decay of a $T_z = -1$ nucleus, or the daughter nucleus in the decay of a $T_Z = 0$ nucleus. The odd-odd nucleus is then treated as a particle-hole excitation built on the even-even Hartree-Fock state. The calculation is carried out in the charge-exchange random-phase approximation (RPA), the lowest-energy state in the RPA spectrum being identified as the isobaric analog state, the state involved in the superallowed β transition. Isospin-symmetry breaking is introduced by the presence of a Coulomb interaction augmented by explicit charge-symmetry-breaking interactions included in the two-body force used in the Hartree-Fock calculation.

First calculations of this type were performed by Sagawa *et al.* [201] with zero-range Skyrme interactions. These were improved upon by Liang *et al.* [202], who replaced zero-range interactions with finite-range meson-exchange potentials in a relativistic rather than nonrelativistic treatment. In a variation of this method, density-dependent meson-nucleon vertices were introduced in a Hartree (only) computation with nonlocal interactions. Liang *et al.* [202] have given results for nine different interactions, out of which we have selected two, labeled PKO1 and DD-ME2, to display in columns 4 and 5 of Table XI. Yet another variant on this technique from Li, Yao, and Chen [203] replaced the finite-range meson-exchange residual interaction with a relativistic point-coupling energy functional in an otherwise identical calculation. One of their results, labeled PC-F1, is given in column 6 of Table XI.

IVMR. A connection between isospin-symmetry breaking and the location of the giant isovector monopole resonance (IVMR) has been demonstrated by Auerbach [204]. This has recently been exploited by Rodin [205] to show that δ_C is related to the reciprocal of the square of an energy parameter that characterizes the IVMR strength distributions. The proportionality coefficient in this relation is determined by basic properties of the ground state of the even-even nucleus and should be reliably calculated in any realistic nuclear model. Rodin gives a few results using an RPA model. These are recorded in column 7 of Table XI.

DFT. The issue of spurious mixing in Hartree-Fock models has been fully addressed in the work of Satula *et al.* [206], who use density functional theory (DFT). They start with a self-consistent Slater-determinant state obtained from a solution of the axially deformed Skyrme-Hartree-Fock equations. That state violates both rotational and isospin symmetries, so their strategy is to restore rotational invariance and remove spurious isospin mixing by a rediagonalization of the Hamiltonian in a basis that conserves those quantities. The numerical effort required to project out good angular momentum and isospin is such that modern Skyrme force parametrizations, which include a density-dependent three-body term, had to be rejected. This effectively left them only one choice: the old Skyrme V (SV) force of Beiner *et al.* [207].

The results from Satula *et al.* [206] produce an unacceptably large correction, $\delta_C \sim 10\%$, for $A = 38$. This they attribute to the poor spectroscopic properties of the SV force which, in this case, shift the energy of the $2s_{1/2}$ subshell to be close to the Fermi surface. A similar effect is probably evident in the $A = 34$ case as well, where a large correction, $\delta_C \sim 1\%$, is obtained. Thus, in recording the DFT results in column 8 of Table XI we have left out the $A = 34$ and 38 cases.

B. CVC test for δ_C corrections

The sets of isospin-symmetry-breaking corrections δ_C recorded in Table XI encompass a wide range of nuclear models and assumptions. Evidently, some test is required to assess the quality of each set and determine its relative merit. The test we use [208] is based on the premise that the CVC hypothesis is valid and thus the corrected $\mathcal{F}t$ values for all measured transitions must be statistically consistent with one another. The success of any calculated set of δ_C values is thus judged by its ability to produce $\mathcal{F}t$ values that are mutually consistent. If we write the average of these $\mathcal{F}t$ values as $\overline{\mathcal{F}t}$, then it follows from Eq. (1) that for each individual transition in the set we can write

$$\delta_C = 1 + \delta_{\rm NS} - \frac{\overline{\mathcal{F}t}}{ft(1+\delta'_R)}. \tag{6}$$

For any set of corrections to be acceptable, the calculated value of δ_C for each transition must satisfy this equation. The test, for a set of δ_C values spanning n superallowed β transitions, is therefore to treat $\overline{\mathcal{F}t}$ as a single adjustable parameter and use it to bring the n results from the right-hand side of Eq. (6), which are based primarily on experiment, into the best possible agreement with the n calculated values of δ_C. The normalized χ^2/ν of the fit, where $\nu = n-1$ is the number of degrees of freedom, then provides a figure of merit.

A few of the sets of δ_C calculations had estimated uncertainties included in their original publications but most did not. So, to be able to test all sets on an equal footing, we have assigned no uncertainties to any of the theoretical δ_C values on the left-hand side of Eq. (6). We do assign uncertainties to the "experimental" quantities on the right-hand side, however. The ft values themselves are taken from Table IX but in some cases their error bars have been slightly reduced: Where an experimental input from Tables I, III, or IV involved

component measurements that were incompatible enough to require a scale factor, we have turned this scale factor off. Our intention is to make the uncertainty on the ft value as purely statistical as possible. The uncertainty on $\delta_{\rm NS}$ is taken from Table X, and that for δ'_R is set at one-third of the order $Z^2\alpha^3$ contribution, as discussed in Sec. III A 1. The χ^2/ν values obtained for each set of δ_C values are given in the last line of Table XI. Note that in testing the DFT calculation, we have dropped the value for ^{62}Ga as it is anomalously low for a heavy-mass nucleus and, if left, would give a far too pessimistic assessment of the overall success of this calculation.

The most obvious outcome of this analysis is that the SM-WS model has a normalized χ^2 smaller by almost a factor of three than any of the other cases cited and is the only one with an acceptable confidence level: 17% compared to <0.01% for all other cases. To illustrate how the alternative models perform, we show in Fig. 5 a plot of the $\mathcal{F}t$ values as determined with two of the alternative models for δ_C used: SM-HF and DFT. A comparison with the bottom panel of Fig. 2, which used the SM-WS model, emphasizes how far the scattered results in Fig. 5 are from agreement with CVC

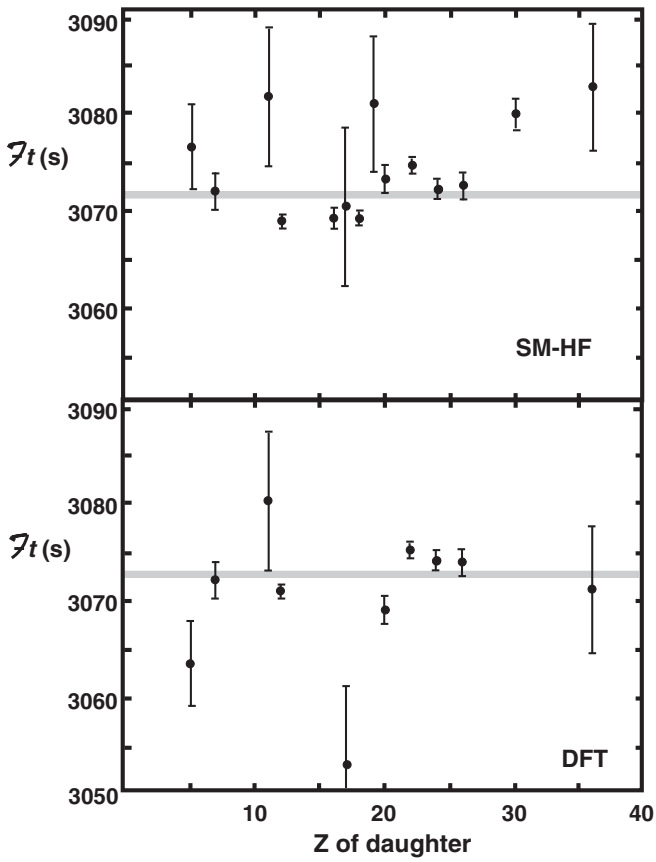

FIG. 5. $\mathcal{F}t$ values as obtained with two alternative models used to calculate δ_C: SM-HF (top) and DFT (bottom). The average $\mathcal{F}t$ value in each case is given by the gray band. The corresponding χ^2/ν for SM-HF is 6.4; for DFT it is 4.3 (see Table XI). Obviously, neither model satisfies the CVC expectation that all $\mathcal{F}t$ values should agree within statistics.

expectations. It is for this reason that the SM-WS δ_C values are the ones we have used to derive the $\mathcal{F}t$ values in Table IX.

C. Mirror test for δ_C corrections

With the recent addition of the β decay of ^{38}Ca [141] to the superallowed data set, an opportunity has been created for the first time to make a high-precision comparison of the ft values from a pair of mirror superallowed decays, $^{38}\text{Ca} \rightarrow {}^{38m}\text{K}$ and $^{38m}\text{K} \rightarrow {}^{38}$ Ar. The ratio of mirror ft values is very sensitive to the model used to calculate the isospin-symmetry-breaking correction, δ_C, and hence serves as another test of the merits of the available calculations.

Starting again with the CVC premise that the corrected $\mathcal{F}t$ values defined in Eq. (1) must be nucleus independent, we can write the ratio of experimental ft values for a pair of mirror superallowed transitions as

$$\frac{ft^a}{ft^b} = 1 + \left(\delta'^b_R - \delta'^a_R\right) + \left(\delta^b_{\rm NS} - \delta^a_{\rm NS}\right) - \left(\delta^b_C - \delta^a_C\right), \qquad (7)$$

where superscript "a" denotes the decay of the $T_z = -1$ parent ($^{38}\text{Ca} \rightarrow {}^{38m}\text{K}$ in the current example) and "b" denotes the mirror decay of the $T_z = 0$ parent ($^{38m}\text{K} \rightarrow {}^{38}\text{Ar}$). The advantage offered by Eq. (7) is that the theoretical uncertainty on the differences $(\delta'^b_R - \delta'^a_R)$, $(\delta^b_{\rm NS} - \delta^a_{\rm NS})$ and $(\delta^b_C - \delta^a_C)$ is significantly less than the uncertainties on the corrections individually for the SM-WS and SM-HF calculations. This is a consequence of the way that these uncertainties were determined. For example, each value for δ_C was taken to be the average of the results obtained from different parameter sets and the quoted "statistical" uncertainty reflected the scatter in those results. If the same approach is used to derive the mirror differences of the correction terms $(\delta^b_C - \delta^a_C)$, the scatter among the results from different parameter sets is less than the scatter observed in either δ^b_C or δ^a_C.

In Table XII we list $(\delta^b_C - \delta^a_C)$ for those cases from Table XI where a value for δ_C is given for both ^{38}Ca and ^{38m}K. In the cases of SM-WS and SM-HF the uncertainty was derived, as just explained, by the same methods as those described

TABLE XII. Values of the calculated difference in the isospin-symmetry-breaking corrections $(\delta^b_C - \delta^a_C)$ in percent units for the mirror β decays of ^{38}Ca and ^{38m}K. Included are all the models listed in Table XI that include a δ_C value for both nuclides. Note that the uncertainties for SM-WS and SM-HF were derived from the model calculations themselves (see text); for the other three models no uncertainties exist, so we assigned them a similar uncertainty. Also listed are the derived ft^a/ft^b ratios and the experimental result. The ft-ratio uncertainties incorporate the contributions from δ'_R, $\delta_{\rm NS}$ and δ_C, although the δ_C uncertainties predominate.

	$\delta^b_C - \delta^a_C$	ft^a/ft^b
SM-WS	−0.095(34)	1.0020(4)
SM-HF	0.125(38)	0.9998(4)
PKO1	−0.035(30)	1.0014(4)
DD-ME2	−0.070(30)	1.0017(4)
PC-F1	−0.053(30)	1.0015(4)
Expt. [141]		1.0036(22)

in the source publications, Refs. [192] and [6]. For the RPA calculations, the source publications list no uncertainties, so we have arbitrarily assigned an uncertainty that is similar to the ones obtained for the shell-model-based calculations. We also list the ratio of ft values obtained from Eq. (7) using $(\delta_R'^b - \delta_R'^a) = 0.026(1)\%$ and $(\delta_{\rm NS}^b - \delta_{\rm NS}^a) = 0.075(20)\%$. For comparison, the experimental result [141] for the ratio appears at the bottom of the column.

The SM-WS and RPA calculations all agree with this result, while the SM-HF calculation differs by two standard deviations. This is immediately attributable to the positive sign that the SM-HF calculation obtains for $(\delta_C^b - \delta_C^a)$, which is unlike the results from all the other model calculations. Intuitively, one expects a negative sign for this difference because nucleus "a" (^{38}Ca in this case) has one more proton than nucleus "b" (^{38m}K), and the Coulomb force is expected to be the dominant influence on the isospin-symmetry breaking. This strongly suggests that there is a problem either with the Hartree-Fock protocol adopted in Ref. [6] or with the degree of spurious isospin mixing that this protocol inevitably includes.

For now, this test can only be applied to the $A = 38$ mirror pair since no other pairs have been completely characterized with the necessary precision. However, every well-known superallowed transitions from a $T_Z = 0$ parent nucleus has a mirror transition from the $T_Z = -1$ member of the same isospin triplet; the latter is simply not fully characterized yet. For two of these $T_Z = -1$ parents, ^{26}Si and ^{34}Ar, the mirror transition only lacks a precise-enough branching-ratio measurement to become useful to test the δ_C calculations. In one more case, that of ^{42}Ti, the half-life and the branching ratio both remain to be determined with sufficient precision. It is likely, though, that all three of these cases will be completed before long [141]. Of course, there are many more possible mirror pairs—with $A = 46,50,54,62,\ldots$—but the $T_Z = -1$ parent nuclei are farther from stability and certainly present a considerable challenge to precise measurement.

V. IMPACT ON WEAK-INTERACTION PHYSICS

A. Value of V_{ud}

We have now tested all available δ_C calculations and demonstrated that only the results from the SM-WS semiphenomenological model satisfy the CVC condition that the corrected $\mathcal{F}t$ values be statistically consistent with one another. It is this set of correction terms that we consequently used to derive the results in Table IX, which led to the value for the average $\overline{\mathcal{F}t}$ and its uncertainty that appears in Eq. (5). In our past two surveys [5,6], we imposed a further systematic uncertainty to account for differences between the two models available at the time to calculate δ_C. Specifically, we calculated the $\mathcal{F}t$ values twice, once with SM-WS and once with SM-HF δ_C values and then averaged the two resulting $\mathcal{F}t$ values together. The added systematic uncertainty was taken to be equal to half the difference between them. But all that happened before we had tests to evaluate the merits of the models.

Not only do we now have such tests, but, in the 6 years since our last survey, new measurements have improved the ft-value data so that the test provides real discrimination. Given the failure of SM-HF to satisfy either the CVC test in Sec. IV B or the mirror test in Sec. IV C, there is no longer any justification to consider it as a viable alternative to the SM-WS model. Furthermore, there is no other model calculation to replace it. Not only do all the other models fail the CVC test but, in fact, not one of them is currently capable of calculating δ_C values for the full set of measured transitions (see Table XI). We therefore now consider the $\overline{\mathcal{F}t}$ value in Eq. (5) to be our final result.

We can now use this result for $\overline{\mathcal{F}t}$ to determine the vector coupling constant, $G_{\rm V}$, from Eq. (1). The value of $G_{\rm V}$ itself is of little interest but, together with the weak-interaction constant for the purely leptonic muon decay, $G_{\rm F}$, it yields the much more interesting up-down element of the CKM quark-mixing matrix. The basic relationship is $V_{ud} = G_{\rm V}/G_{\rm F}$, which in terms of $\overline{\mathcal{F}t}$ becomes

$$|V_{ud}|^2 = \frac{K}{2G_{\rm F}^2(1+\Delta_{\rm R}^{\rm V})\overline{\mathcal{F}t}} = \frac{2915.64 \pm 1.08}{\overline{\mathcal{F}t}}, \quad (8)$$

where we have used the MuLan [185,209] value for the weak-interaction coupling constant from muon decay, $G_{\rm F}/(\hbar c)^3 = 1.166\,378\,7(6) \times 10^{-5}\,{\rm GeV}^{-2}$; the value for $\Delta_{\rm R}^{\rm V}$, the nucleus-independent radiative correction, is taken from Eq. (3). Substituting the result for $\overline{\mathcal{F}t}$ from Eq. (5), we obtain

$$|V_{ud}|^2 = 0.949\,00 \pm 0.000\,42. \quad (9)$$

Note that the total uncertainty here is almost entirely due to the uncertainties contributed by the theoretical corrections. By far the largest contribution, 0.000 35, arises from the uncertainty in $\Delta_{\rm R}^{\rm V}$; 0.000 18 comes from the nuclear-structure-dependent corrections $(\delta_C - \delta_{\rm NS})$, and 0.000 11 is attributable to δ_R'. Only 0.000 09 can be considered to be experimental in origin. The latter contribution has decreased by nearly a factor of two since our last survey but, because of the dominance of the theoretical uncertainties, which have not changed significantly, the overall improvement in $|V_{ud}|^2$ is much less pronounced.

The corresponding value of V_{ud} is

$$|V_{ud}| = 0.974\,17(21), \quad (10)$$

a result which is consistent with, but a bit more precise than, values we have obtained in previous analyses of superallowed β decay. To emphasize the consistency and steady improvement that has characterized the value of V_{ud} as derived from nuclear β decay, in Fig. 6 we plot our new result together with V_{ud} values published at various times over the past two and a half decades [4–6,210,211].

B. Value of V_{us}

The recommended value for V_{us}, the second largest top-row element of the CKM matrix, is derived from the decays, both leptonic and semileptonic, of the kaon. Other determinations based on hyperon decays and hadronic τ decays, which do

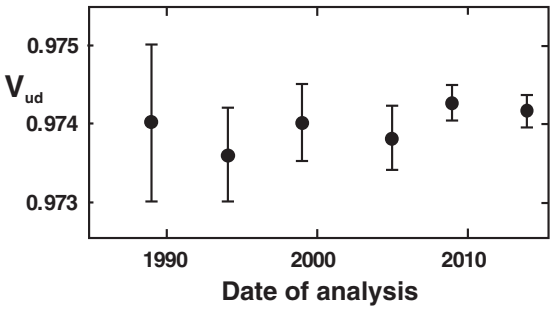

FIG. 6. Values of V_{ud} as determined from superallowed $0^+ \rightarrow 0^+$ β decays plotted as a function of analysis date, spanning the past two and a half decades. In order, from the earliest date to the most recent, the values are taken from Refs. [4], [210], [211], [5], [6], and this work.

not currently have sufficient precision to challenge the results from kaon decays, are not considered here.

For the semileptonic $K \rightarrow \pi \ell \nu_\ell$ ($K_{\ell 3}$) decays, there are four separate decay channels that may be studied: charged kaons or neutral kaons (long or short) decaying to either electrons or muons. Results from these experiments have been evaluated by the FlaviaNet group [212], with updates discussed at the CKM14 conference by Moulson [213]. Extracted from the experimental data is the product

$$f_+(0)|V_{us}| = 0.2165(4), \tag{11}$$

where $f_+(0)$ is the semileptonic-decay form factor at zero-momentum transfer. Its value is close to unity. In the exact SU(3) symmetry limit, the CVC hypothesis would require its value to be exactly one but, in $K_{\ell 3}$ decays, SU(3) symmetry is broken at second order and a theoretical calculation is required to estimate the extent of the symmetry breaking. Today, lattice QCD calculations are used for this purpose, replacing former semianalytic methods based on chiral perturbation theory.

For purely leptonic kaon decays, $K^\pm \rightarrow \mu^\pm \nu$ ($K_{\ell 2}$), it is their ratio to leptonic pion decays, $\pi^\pm \rightarrow \mu^\pm \nu$, that is measured because hadronic uncertainties can be minimized in the ratio. The resulting experimental output is the ratio of CKM matrix elements $|V_{us}|/|V_{ud}|$ multiplied by the ratio of decay constants f_K/f_π. The current recommended value from Moulson [213] is

$$\frac{f_K}{f_\pi}\frac{|V_{us}|}{|V_{ud}|} = 0.2760(4). \tag{12}$$

Again a lattice QCD calculation is required to evaluate the ratio of decay constants.

In the past few years, there has been a rapid expansion in large-scale numerical simulations in lattice QCD aimed at determining the low-energy constants of flavor physics. A Flavor Lattice Averaging Group (FLAG) formed in 2007 has been enlarged and the first report from the expanded group has just been released [214]. Their recommended values for the low-energy constants depend on N_f, the number of dynamical quark flavors included in the lattice simulations. The earliest results with $N_f = 2$ included just up and down quarks; more recently strange quarks were added, so those calculations are designated by $N_f = 2 + 1$. Most recently, calculations with $N_f = 2 + 1 + 1$ have been reported, in which charm quarks are incorporated as well. The FLAG group gives results separately for $N_f = 2$, $N_f = 2 + 1$, and $N_f = 2 + 1 + 1$, arguing that they have no *a priori* way to estimate quantitatively the differences among results produced in simulations with different numbers of dynamical quarks.

In Table XIII we give recommended values for $f_+(0)$ and f_K/f_π that lead to values of $|V_{us}|$ in rows 1 to 3 and $|V_{us}|/|V_{ud}|$ in rows 4 to 6. The entries for $N_f = 2$ and $N_f = 2 + 1$ are the FLAG averages from [214]. Those for $N_f = 2 + 1 + 1$

TABLE XIII. Lattice QCD values for $f_+(0)$ and f_K/f_π appear in columns 2 and 3, respectively, distinguished by the number of quark flavors present in the simulations. The values corresponding to $N_f = 2$ and $N_f = 2 + 1$ are averages taken from FLAG [214]. The results for $N_f = 2 + 1 + 1$ are from more recent publications [215,216]. The deduced values of $|V_{us}|$ (for $K_{\ell 3}$ decays) and those of $|V_{us}|/|V_{ud}|$ (for $K_{\ell 2}$ decays) appear in columns 4 and 5, respectively. The unitarity sums in column 6 incorporate V_{ud} from Eq. (10) and V_{ub} from Eq. (14). Their residuals, $\Delta_{\rm CKM}$, are in column 7 and, if unitarity is not met within the quoted uncertainty, the number of standard deviations, σ, of the discrepancy appears in column 8. Rows 7 to 9 give $|V_{us}|$ obtained by our fitting three data—$|V_{ud}|$ from β decay, $|V_{us}|$ from $K_{\ell 3}$ decays, and $|V_{us}|/|V_{ud}|$ from $K_{\ell 2}$ decays—with two free parameters, $|V_{ud}|$ and $|V_{us}|$, for each of the specified values of N_f. The Particle Data Group $|V_{us}|$ value [185] is given in the last row.

	$f_+(0)$	f_K/f_π	$\lvert V_{us}\rvert$	$\lvert V_{us}\rvert/\lvert V_{ud}\rvert$	$\lvert V_u\rvert^2$	$\Delta_{\rm CKM}$	σ
$N_f = 2 + 1 + 1$	0.9704(32)[a]		0.2232(9)		0.9988(6)	−0.0012(6)	2.1
$N_f = 2 + 1$	0.9661(32)		0.2241(9)		0.9992(6)	−0.0008(6)	1.4
$N_f = 2$	0.9560(84)		0.2265(20)		1.0003(10)	0.0003(10)	
$N_f = 2 + 1 + 1$		1.1960(25)[b]		0.2308(6)	0.9996(5)	−0.0004(5)	
$N_f = 2 + 1$		1.192(5)		0.2315(10)	0.9999(6)	−0.0001(6)	
$N_f = 2$		1.205(18)		0.2290(34)	0.9988(15)	−0.0012(15)	
$N_f = 2 + 1 + 1$			0.2243(8)		0.9993(8)	−0.0007(8)	
$N_f = 2 + 1$			0.2247(7)		0.9995(6)	−0.0005(6)	
$N_f = 2$			0.2256(17)		0.9999(9)	−0.0001(9)	
PDG 14			0.2253(8)		0.9998(6)	−0.0002(6)	

[a]This recent result from Ref. [215] replaces the FLAG average [214], which is less precise.
[b]This recent result from Ref. [216] with symmetrized uncertainty replaces the FLAG average [214], which is less precise.

are more recent results [215,216], which appeared after the deadline for inclusion in the FLAG averages. Since they are more precise than the FLAG averages, we have followed Moulson [213] in using them instead.

With $|V_{us}|$ from rows 1 to 3, $|V_{us}|/|V_{ud}|$ from rows 4 to 6, and $|V_{ud}|$ from superallowed β decay as given in Eq. (10), we have three pieces of data from which to determine two parameters, $|V_{ud}|$ and $|V_{us}|$. To do so, we performed nonlinear least-squares fits to obtain the values of $|V_{us}|$ given in rows 7 to 9 in Table XIII. Note that the χ^2 of these three fits were 2.6, 1.2, and <1, respectively, so the uncertainties shown for the first two $|V_{us}|$ values have been scaled appropriately. The corresponding value of $|V_{ud}|$ in each case undergoes very little change from its input value, although its uncertainty increases: For the $N_f = 2+1+1$ case, its central value shifts by two units in the last digit quoted, to 0.974 15(34); for $N_f = 2+1$, it shifts by one unit, to 0.974 16(23); and for $N_f = 2$, there is no change at all.

In the last line of the Table XIII we give the most up-to-date Particle Data Group (PDG) value [217] for $|V_{us}|$, which was arrived at without the very recent $N_f = 2+1+1$ lattice calculations [215,216]. To obtain their average result, the PDG used $|V_{us}| = 0.2253(14)$ from their analysis of $K_{\ell 3}$ decays, and $|V_{us}|/|V_{ud}| = 0.2313(10)$ from the leptonic decays of kaons and pions. Note that both values are statistically consistent with all the results for the same quantities given in rows 1–3 and 4–6. The same can be said for the comparison of the average PDG result for $|V_{us}|$ on the bottom line with our fitted results on the three lines above it.

C. CKM unitarity

The standard model does not prescribe the individual elements of the CKM matrix—they must be determined experimentally—but absolutely fundamental to the model is the requirement that the matrix be unitary. To date, the most demanding test of CKM unitarity comes from the sum of the squares of the top-row elements,

$$|V_u|^2 \equiv |V_{ud}|^2 + |V_{us}|^2 + |V_{ub}|^2 = 1 + \Delta_{\rm CKM}, \qquad (13)$$

which should equal exactly one: i.e., the residual, $\Delta_{\rm CKM}$, should be exactly zero. Because $|V_{ud}|^2$ accounts for 95% of this sum, its precision (and accuracy) is of paramount importance. Our analysis in this survey demonstrates that the current value for $|V_{ud}|$ given in Eq. (10) is solidly based on a robust body of diverse data and, although its precision has improved continuously, it has not shifted outside of previously quoted error bars in a quarter century. It now has a precision of 0.02%, which makes it the most precisely determined element in the CKM matrix by far.

Values for $|V_{us}|$ discussed in Sec. V B and shown in Table XIII typically have a quoted precision of 0.4%, of which approximately one-third is experimental and two-thirds theoretical, the latter arising from the precision attained in recent lattice QCD simulations. The third element of the top row, V_{ub}, is very small and hardly impacts on the unitarity test at all. Its value from the PDG compilation [185] is

$$|V_{ub}| = (4.15 \pm 0.49) \times 10^{-3}. \qquad (14)$$

Our approach to the unitarity test in the past has always been to combine our result for $|V_{ud}|$ with the PDG evaluated results for $|V_{us}|$ and $|V_{ub}|$. If we do that—taking $|V_{ud}|$ from Eq. (10), $|V_{us}|$ from the bottom line of Table XIII and $|V_{ub}|$ from Eq. (14)—we obtain the result

$$|V_u|^2 = 0.999\,78 \pm 0.000\,55. \qquad (15)$$

But this cannot be the final word since the PDG evaluation does not include results from the most recent lattice calculations, which are used to extract $|V_{us}|$ and $|V_{us}|/|V_{ud}|$ from kaon-decay measurements.

So how well is the unitarity relation satisfied if the new results are included? In what follows we take $|V_{ud}|$ solely from Eq. (10) and $|V_{ub}|$ from Eq. (14). We then examine how unitarity depends on the possible choices for $|V_{us}|$. First, from Table XIII we can see that if $|V_{us}|$ is determined solely from $K_{\ell 3}$ experiments, then successive improvements in lattice calculations have led to increasing values of $f_+(0)$ and steadily smaller values of $|V_{us}|$ (see rows 1–3). This has led to increasing tension with unitarity. The most recent lattice calculation with $N_f = 2+1+1$ quark flavors by Bazavov *et al.* [215] leaves unitarity unsatisfied by 2.1 standard deviations. This is certainly a provocative outcome. Even with only $N_f = 2+1$ flavors in the calculation there is some tension, with $\Delta_{\rm CKM}$ being 1.4 standard deviations away from zero.

By contrast, $K_{\ell 2}$ experiments yielding the ratio $|V_{us}|/|V_{ud}|$ and a unitarity sum calculated via

$$|V_u|^2 = |V_{ud}|^2 \left(1 + \left|\frac{V_{us}}{V_{ud}}\right|^2\right) + |V_{ub}|^2 = 1 + \Delta_{\rm CKM}, \qquad (16)$$

agree perfectly with unitarity regardless of the number of quark flavors in the decay-constant calculation (see rows 4–6).

Evidently, there is some incompatibility between the $|V_{us}|$ value determined from $K_{\ell 3}$ decays and that determined from $K_{\ell 2}$ decays. Even so, one possible way forward is to combine the $K_{\ell 3}$ and $K_{\ell 2}$ results to arrive at a compromise value for $|V_{us}|$. This we have done, with the results appearing in rows 7–9 in Table XIII. The unitarity test is satisfied for all three cases but this has come at a price: For the more modern lattice calculations, the uncertainties have been increased.

Now let us examine a number of specific scenarios.

(1) Kaon experiments correct, unitarity satisfied. Accepting that Eqs. (11) and (12) are correct and $|V_u|^2 = 1$, we can solve for $f_+(0)$ and f_K/f_π to obtain $f_+(0) = 0.9590(43)$ and $f_K/f_\pi = 1.191(5)$. These values agree with all lattice calculations for f_K/f_π, but only agree with the older $N_f = 2$ results for $f_+(0)$.

(2) f_K/f_π correct, $K_{\ell 2}$ experiment correct, unitarity satisfied. Accepting the $N_f = 2+1+1$ value for f_K/f_π and the $K_{\ell 2}$ result in Eq. (12), we can solve for $|V_{ud}|$, obtaining $|V_{ud}| = 0.974\,38(12)$, which agrees with the superallowed β-decay result in Eq. (10). Clearly, the $K_{\ell 2}$ data and corresponding lattice calculations are fully compatible with nuclear β decay and unitarity.

(3) $f_+(0)$ correct, $K_{\ell 3}$ correct, unitarity satisfied. Given the $N_f = 2+1+1$ value for $f_+(0)$ and the $K_{\ell 3}$ experimental result in Eq. (11), we can solve for $|V_{ud}|$, obtaining $|V_{ud}| = 0.974\,77(20)$, which differs from the β-decay value by 2.1

standard deviations. Is there any way the $|V_{ud}|$ value in Eq. (10) could possibly be shifted to this value? It can be seen in Eq. (8) that $|V_{ud}|^2$ is inversely proportional to both $\overline{\mathcal{F}t}$ and $(1+\Delta_R^V)$. For $\overline{\mathcal{F}t}$ to account for such a shift, it would have to decrease by six standard deviations. That is unlikely enough but, because all 14 measured transitions agree with one another and with CVC, all 14 would have to undergo the same shift, a virtual impossibility. The only other possibility is a shift in the nucleus-independent radiative correction, Δ_R^V, which would have to be reduced from 2.36(4)% to 2.24%. This is a change equal to three times the stated uncertainty which, while not impossible, is rather unlikely.

(4) $f_+(0)$, f_K/f_π correct, $K_{\ell 3}$, $K_{\ell 2}$ correct, unitarity not satisfied. With $|V_{us}|$ determined from $K_{\ell 3}$ decays and $|V_{us}|/|V_{ud}|$ from $K_{\ell 2}$ decays, each with the $N_f = 2+1+1$ lattice coupling constants, a value of $|V_{ud}|$ can be obtained from their ratio. The result, $|V_{ud}| = 0.9670(44)$, has a somewhat larger error bar than other determinations from kaon physics because no constraint to satisfy unitarity has been imposed. Nevertheless, the result is two of its standard deviations away from the nuclear β-decay value for $|V_{ud}|$ and the unitarity sum is likewise not satisfied, with $|V_u|^2 = 0.985(9)$ and a deficit, $\Delta_{CKM} = -0.015(9)$, of 1.8 standard deviations. For the β-decay value of $|V_{ud}|$ to be shifted into agreement with this kaon-derived value would require the nucleus-independent radiative correction Δ_R^V to be increased from 2.36(4)% to 3.88%, 40 times its stated uncertainty. Surely this can be ruled out.

One must conclude that there is no definitive answer for $|V_{us}|$ as of now since the two approaches to its measurement from kaon decay are not completely consistent with one another. On balance, though, the result for $|V_{us}|/|V_{ud}|$ obtained from $K_{\ell 2}$ and pion decays seems the most reliable because it shows the greatest consistency as the lattice calculations have improved, which reinforces the idea that systematic errors are reduced when a ratio is used. If we then accept the $N_f = 2+1+1$ result on line 4 of Table XIII and combine it with our result for $|V_{ud}|$ from Eq. (10), we get $|V_{us}| = 0.2248(6)$ and a unitary sum of $|V_u|^2 = 0.999\,56(49)$.

D. Scalar currents

1. Fundamental scalar current

The standard model prescribes the weak interaction to be an equal mix of vector (V) and axial-vector (A) interactions that maximizes parity violation. Searches for physics beyond the standard model therefore seek evidence that parity is not maximally violated (owing to the presence of right-hand currents) or that the interaction is not pure $V-A$ (owing to the presence of scalar or tensor currents). The data in this survey allow us to contribute to the search for a scalar interaction because, if present, it would have a measurable effect on superallowed $0^+ \to 0^+$ β transitions.

A scalar interaction would generate an additional term [5] to the shape-correction function, which forms part of the integrand of the statistical rate function, f, an integral over the β-decay phase space. The additional term takes the form $(1 + b_F \gamma_1 / W)$, where W is the total electron energy in electron rest-mass units, and $\gamma_1 = \sqrt{[1-(\alpha Z)^2]}$. The strength of the scalar interaction is contained in the unknown constant, b_F, which is called the Fierz interference term [218]. Thus, the impact of a scalar interaction on the $\mathcal{F}t$ values would be to introduce a dependence on $\langle 1/W \rangle$, the average inverse decay energy of each β^+ transition. No longer would the $\mathcal{F}t$ values be constant over the whole range of nuclei but they would instead exhibit a smooth dependence on $\langle 1/W \rangle$. Since $\langle 1/W \rangle$ is largest for the lightest nuclei, and decreases monotonically with increasing Z and A, the largest deviation of $\mathcal{F}t$ from constancy would occur for the cases of ^{10}C and ^{14}O.

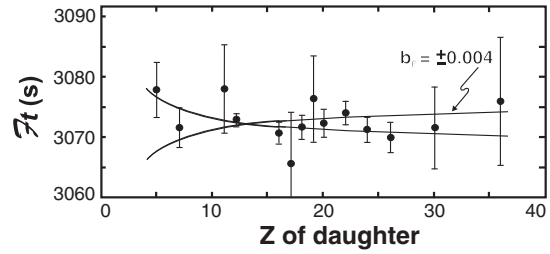

FIG. 7. Corrected $\mathcal{F}t$ values from Table IX plotted as a function of the charge on the daughter nucleus, Z. The curved lines represent the approximate loci the $\mathcal{F}t$ values would follow if a scalar current existed with $b_F = \pm 0.004$.

We have reevaluated the statistical rate function, f, for each transition using a shape-correction function that includes the presence of the scalar interaction via a Fierz interference term, b_F, which we treat as an adjustable parameter. We then obtained a value of b_F that minimized the χ^2 in a least-squares fit to the expression $\mathcal{F}t =$ constant. The result we obtained is

$$b_F = -0.0028 \pm 0.0026, \tag{17}$$

a marginally larger result than the value from our last survey [6] but with the same uncertainty. Note that the uncertainty quoted here is one standard deviation (68% CL), as obtained from the fit. In Fig. 7 we illustrate the sensitivity of this analysis by plotting the measured $\mathcal{F}t$ values together with the loci of $\mathcal{F}t$ values that would be expected if $b_F = \pm 0.004$. There is no statistically compelling evidence for b_F to be nonzero.[1]

The result in Eq. (17) can also be expressed in terms of the coupling constants that Jackson, Treiman, and Wyld [218] introduced to write a general form for the weak-interaction Hamiltonian. Since we are dealing only with Fermi superallowed transitions, we can restrict ourselves to scalar and vector couplings, for which the Hamiltonian becomes

$$H_{S+V} = (\overline{\psi}_p \psi_n)\left(C_S \overline{\phi}_e \phi_{\overline{\nu}_e} + C_S' \overline{\phi}_e \gamma_5 \phi_{\overline{\nu}_e}\right) + (\overline{\psi}_p \gamma_\mu \psi_n)\left[C_V \overline{\phi}_e \gamma_\mu (1+\gamma_5)\phi_{\overline{\nu}_e}\right], \tag{18}$$

in the notation and metric of Ref. [218]. We have taken the vector current to be maximally parity violating, as indicated

[1] It is interesting to note that if we were to derive an average $\overline{\mathcal{F}t}$ value from the data while allowing b_F to vary freely, the corresponding value for $|V_{ud}|$ would become 0.9745(4), a result quite consistent with the one we quote in Eq. (10), but with an uncertainty nearly twice as large.

by experiment. The complexity of the relationship between b_F and the couplings C_S, C'_S, and C_V depends on what assumptions are made about the properties of the scalar current. If we take the most restrictive conditions, that the scalar and vector currents are time-reversal invariant (i.e., C_S and C_V are real) and that the scalar current, like the vector current, is maximally parity violating (i.e., $C_S = C'_S$), then we can write[2]

$$\frac{C_S}{C_V} = -\frac{b_F}{2} = +0.0014 \pm 0.0013. \tag{19}$$

This limit from superallowed β decay is, by far, the tightest limit available on the presence of a scalar current under the assumptions stated.

If we remove the condition that the scalar current be maximally parity violating, then the expression contains two unknowns,

$$b_F = \frac{-2C_V(C_S + C'_S)}{2|C_V|^2 + |C_S|^2 + |C'_S|^2} \simeq -\left(\frac{C_S}{C_V} + \frac{C'_S}{C_V}\right), \tag{20}$$

and cannot be solved individually for C_S/C_V and C'_S/C_V. However, the β-ν angular-correlation coefficient, a, for a superallowed $0^+ \to 0^+$ β transition provides another independent measure of C_S and C_V. In that case,

$$a = \frac{2|C_V|^2 - |C_S|^2 - |C'_S|^2}{2|C_V|^2 + |C_S|^2 + |C'_S|^2} \simeq 1 - \left(\frac{|C_S|^2}{|C_V|^2} + \frac{|C'_S|^2}{|C_V|^2}\right), \tag{21}$$

which, together with Eq. (20), can be used to set limits on both C_S/C_V and C'_S/C_V.

In our previous survey [6] we combined our result for b_F with the result from a β-ν correlation measurement in the superallowed emitter ^{38m}K [219]. Our new value for b_F in Eq. (17) is so little changed from our previous one that we quote the same 68% confidence limits for C_S/C_V and C'_S/C_V, viz.,

$$\frac{|C_S|}{|C_V|} \leqslant 0.065, \quad \frac{|C'_S|}{|C_V|} \leqslant 0.065. \tag{22}$$

The reader is referred to Fig. 8 in Ref. [6] for a visual representation of these results and their derivation.

A review of the limits obtained on exotic weak-interaction couplings from precision β-decay experiments has recently been produced by Naviliat-Cuncic and González-Alonso [220].

2. *Induced scalar currents*

If we consider only the vector part of the weak interaction for composite spin-$\frac{1}{2}$ nucleons, then the most general form the interaction can take is written [221]

$$H_V = \overline{\psi}_p(g_V\gamma_\mu - f_M\sigma_{\mu\nu}q_\nu + if_S q_\mu)\psi_n\overline{\phi}_e\gamma_\mu(1+\gamma_5)\phi_{\overline{\nu}_e}, \tag{23}$$

with q_μ being the four-momentum transfer between hadrons and leptons. The values of the coupling constants g_V (vector), f_M (weak magnetism), and f_S (induced scalar) are predetermined if the CVC hypothesis—that the weak vector current is just an isospin rotation of the electromagnetic vector current—is correct. In particular, because CVC implies that the vector current is divergenceless, the induced scalar term f_S should be identically zero. With the data from superallowed β decay it is possible to test this prediction of CVC by setting an experimental limit on the value of f_S.

We showed in Ref. [5] that the Hamiltonian in Eq. (23) can be reorganized to match exactly the form given by Jackson, Treiman, and Wyld [Eq. (18)], with C_S simply replaced with $m_e f_S$ and C_V with g_V. Here m_e is the electron rest mass, which is $m_e = 1$ in electron rest-mass units. Thus, the value for C_S/C_V in Eq. (19) applies equally well to the ratio $m_e f_S/g_V$. Expressed as a limit at the 90% confidence level, we obtain

$$\left|\frac{m_e f_S}{g_V}\right| < 0.0035. \tag{24}$$

This result is a vindication for the CVC hypothesis that predicts $g_V = 1$ and $f_S = 0$. Our 90% confidence limit confirms this prediction at the level of 35 parts in 10^4.

VI. CONCLUSIONS

It has been 6 years since our previous survey of superallowed $0^+ \to 0^+$ β decay. In that time, substantial progress has been made both in improving the precision of previously measured ft values and in adding a new transition, a particularly interesting one that completes for the first time a mirror pair of $0^+ \to 0^+$ transitions, ^{38}Ca $\to$ ^{38m}K and ^{38m}K $\to$ ^{38}Ar. The principal outcome of the new data is to have improved our ability to discriminate among the various calculations of the isospin-symmetry-breaking correction, δ_C. This is an important step forward, because these correction terms contribute more to the overall uncertainty on $|V_{ud}|^2$ than do the experimental measurements themselves. Even so, neither is the biggest contributor to the $|V_{ud}|^2$ uncertainty.

It is instructive to look at the complete uncertainty budget for $|V_{ud}|^2$ in Fig. 8, where the four major contributions are displayed in units of parts in 10^4. By now, experiment has completely outstripped theory in its remarkable precision. However, just as important as its precision is the fact that it includes more than 220 independent measurements covering 14 separate transitions, each with a $Q_{\rm EC}$ value, half-life, and branching ratio that has been determined, in most cases, multiple times. What is more, all 14 transitions yield $\mathcal{F}t$ values that are statistically consistent with one another. This is indeed a robust body of data, completely insensitive to the possible presence of a few aberrant measurements.

As Fig. 8 makes clear, by far the largest contributor to the $|V_{ud}|^2$ uncertainty is the calculated radiative correction $\Delta_{\rm R}^{\rm V}$. If any real improvement in the unitarity test from $0^+ \to 0^+$ β

[2]More correctly we would write $C_S/C_V = \pm b_F/2$, with the upper sign for β^- transitions and the lower sign for β^+ transitions. Because all the superallowed Fermi transitions are positron emitters, we display only the lower sign in our equations. The sign change comes about because $\overline{\psi}_p C_S \psi_n$ changes sign under charge conjugation relative to $\overline{\psi}_p C_V \gamma_4 \psi_n$.

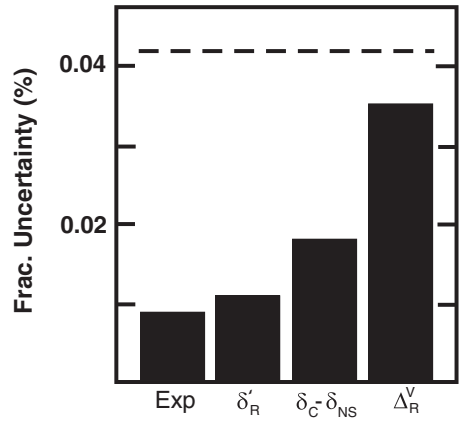

FIG. 8. Uncertainty budget for $|V_{ud}|^2$ as obtained from superallowed $0^+ \rightarrow 0^+$ β decay. The contributions are separated into four categories: experiment, the transition-dependent part of the radiative correction (δ'_R), the nuclear-structure-dependent terms ($\delta_C - \delta_{NS}$), and the transition-independent part of the radiative correction Δ^V_R.

decay is to be achieved in the future, it must come first from improved calculations of Δ^V_R. Furthermore, since Δ^V_R is common to all other approaches to the measurement of $|V_{ud}|$—from neutron decay, $T = 1/2$ nuclear mirror decays and pion decays—it provides an ultimate precision limit to them all, albeit well below the experimental uncertainties which currently dominate those measurements. In 2008, we identified improvements to Δ^V_R as the highest priority theoretical goal, and it remains so today. The impact of any improvement would be immediate: If the Δ^V_R uncertainty were cut in half, the $|V_{ud}|^2$ uncertainty would be reduced by 30%.

The nuclear-structure-dependent corrections ($\delta_C - \delta_{NS}$) are the second most important contributors to the overall uncertainty assigned to $|V_{ud}|^2$. Their contribution has been slightly reduced since 2008 as a result of improved experimental precision which, as already noted, has made possible a discriminating test for the efficacy of any set of calculated isospin-symmetry-breaking corrections, δ_C. As a result, we have been able to select the only set in good agreement with the expectation of CVC that all measured transitions should have the same $\mathcal{F}t$ values within statistical uncertainties. This is an example of experiment contributing to the reduction of a theoretical uncertainty. Further benefits from the same approach can also be anticipated in the future with the completion of more mirror pairs of $0^+ \rightarrow 0^+$ transitions—at $A = 26$, 34, and 42, for example—and with even higher precision in the already well-known ft values.

Of course, the motivation for improving $|V_{ud}|$ is to tighten the uncertainty on CKM unitarity as a probe for physics beyond the standard model. This would obviously benefit from a resolution of the current conflict in the determinations of $|V_{us}|$. Nevertheless, regardless of which current value for $|V_{us}|$ one accepts, its contribution to the uncertainty on the unitarity sum is from 15%–35% less than that of our current value of $|V_{ud}|$. (The *relative* precision of $|V_{ud}|$ is, however, more than an order of magnitude tighter than that of $|V_{us}|$.) Thus, any improvement in $|V_{ud}|$ will have a direct beneficial impact on the uncertainty of the unitarity sum.

There is another important outcome of the superallowed $\mathcal{F}t$ values that often gets less attention than it deserves: the experimental limit that it yields on the possible occurrence of a scalar interaction. The limit set here on the ratio of scalar-to-vector currents is the tightest available anywhere and it can clearly be improved. As a glance at Fig. 7 will show, the two lightest superallowed transitions—those from ^{10}C and ^{14}O—are crucial in setting the limit on a scalar interaction. Both have relatively large uncertainties. Both also present experimental challenges, particularly in the measurement of their branching ratios. There is no doubt, though, that an appreciable improvement in their $\mathcal{F}t$ values would pay off handsomely.

ACKNOWLEDGMENTS

This material is based upon work supported by the U.S. Department of Energy, Office of Science, Office of Nuclear Physics, under Award No. DE-FG03-93ER40773 and by the Welch Foundation under Grant No. A-1397.

[1] I. S. Towner and J. C. Hardy, Nucl. Phys. A **205**, 33 (1973).
[2] J. C. Hardy and I. S. Towner, Nucl. Phys. A **254**, 221 (1975).
[3] V. T. Koslowsky, E. Hagberg, J. C. Hardy, H. Schmeing, R. E. Azuma, and I. S. Towner, in *Proceedings of the 7th International Conference on Atomic Masses and Fundamental Constants, Darmstadt-Seeheim*, edited by O. Klepper (T. H. Darmstadt, Darmstadt, Germany, 1984), p. 572.
[4] J. C. Hardy, I. S. Towner, V. T. Koslowsky, E. Hagberg, and H. Schmeing, Nucl. Phys. A **509**, 429 (1990).
[5] J. C. Hardy and I. S. Towner, Phys. Rev. C **71**, 055501 (2005); Phys. Rev. Lett. **94**, 092502 (2005).
[6] J. C. Hardy and I. S. Towner, Phys. Rev. C **79**, 055502 (2009).
[7] E. G. Adelberger, M. M. Hindi, C. D. Hoyle, H. E. Swanson, R. D. Von Lintig, and W. C. Haxton, Phys. Rev. C **27**, 2833 (1983); this reference replaces the result reported in E. G. Adelberger, C. D. Hoyle, H. E. Swanson, and R. D. Von Lintig, Phys. Rev. Lett. **46**, 695 (1981).
[8] F. Ajzenberg-Selove, Nucl. Phys. A **490**, 1 (1988).
[9] F. Ajzenberg-Selove, Nucl. Phys. A **523**, 1 (1991).
[10] A. M. Aldridge, K. W. Kemper, and H. S. Plendl, Phys. Lett. B **30**, 165 (1969).
[11] D. E. Alburger, Phys. Rev. C **5**, 274 (1972).
[12] D. E. Alburger and F. P. Calaprice, Phys. Rev. C **12**, 1690 (1975).
[13] D. E. Alburger and D. H. Wilkinson, Phys. Rev. C **15**, 2174 (1977); this reference replaces the ^{46}V half-life from [181].
[14] D. E. Alburger, Phys. Rev. C **18**, 1875 (1978).
[15] P. F. A. Alkemade, C. Alderliesten, P. De Wit, and C. Van der Leun, Nucl. Instrum. Methods **197**, 383 (1982).
[16] A. Anttila, M. Bister, and E. Arminen, Z. Phys. **234**, 455 (1970).

[17] G. Azuelos, J. E. Crawford, and J. E. Kitching, Phys. Rev. C **9**, 1213 (1974).
[18] G. Azuelos and J. E. Kitching, Phys. Rev. C **12**, 563 (1975).
[19] R. K. Bardin, C. A. Barnes, W. A. Fowler, and P. A. Seeger, Phys. Rev. **127**, 583 (1962).
[20] P. H. Barker, C. J. Scofield, R. J. Petty, J. M. Freeman, S. D. Hoath, W. E. Burcham, and G. T. A. Squier, Nucl. Phys. A **275**, 37 (1977); the same result also appears in G. T. A. Squier, W. E. Burcham, S. D. Hoath, J. M. Freeman, P. H. Barker, and R. J. Petty, Phys. Lett. B **65**, 122 (1976).
[21] P. H. Barker and J. A. Nolen, *Proceedings of the International Conference on Nuclear Structure, Tokyo, Japan* (International Academic Printing Co, Ltd., Tokyo, 1977).
[22] P. H. Barker and R. E. White, Phys. Rev. C **29**, 1530 (1984).
[23] P. H. Barker and S. M. Ferguson, Phys. Rev. C **38**, 1936 (1988).
[24] S. C. Baker, M. J. Brown, and P. H. Barker, Phys. Rev. C **40**, 940 (1989).
[25] P. H. Barker and G. D. Leonard, Phys. Rev. C **41**, 246 (1990).
[26] P. H. Barker and P. A. Amundsen, Phys. Rev. C **58**, 2571 (1998); this reference updates the ^{10}C Q_{EC} value from [24]; its value for the ^{14}O Q_{EC} value was later withdrawn in [171].
[27] P. H. Barker and M. S. Wu, Phys. Rev. C **62**, 054302 (2000).
[28] G. C. Ball, S. Bishop, J. A. Behr, G. C. Boisvert, P. Bricault, J. Cerny, J. M. D'Auria, M. Dombsky, J. C. Hardy, V. Iacob, J. R. Leslie, T. Lindner, J. A. Macdonald, H.-B. Mak, D. M. Moltz, J. Powell, G. Savard, and I. S. Towner, Phys. Rev. Lett. **86**, 1454 (2001).
[29] P. H. Barker, I. C. Barnett, G. J. Baxter, and A. P. Byrne, Phys. Rev. C **70**, 024302 (2004).
[30] P. H. Barker and A. P. Byrne, Phys. Rev. C **73**, 064306 (2006).
[31] P. H. Barker, K. K. H. Leung, and A. P. Byrne, Phys. Rev. C **79**, 024311 (2009).
[32] G. C. Ball, G. Boisvert, P. Bricault, R. Churchman, M. Dombsky, T. Lindner, J. A. Macdonald, E. Vandervoort, S. Bishop, J. M. D'Auria, J. C. Hardy, V. E. Iacob, J. R. Leslie, and H.-B. Mak, Phys. Rev. C **82**, 045501 (2010).
[33] E. Beck and H. Daniel, Z. Phys. **216**, 229 (1968).
[34] J. A. Becker, R. A. Chalmers, B. A. Watson, and D. H. Wilkinson, Nucl. Instrum. Methods **155**, 211 (1978).
[35] F. J. Bergmeister, K. P. Lieb, K. Pampus, and M. Uhrmacher, Z. Phys. A **320**, 693 (1985).
[36] A. Bey *et al.*, Eur. Phys. J. A **36**, 121 (2008).
[37] S. Bishop *et al.*, Phys. Rev. Lett. **90**, 162501 (2003).
[38] B. Blank, G. Savard, J. Doring, A. Blazhev, G. Canchel, M. Chartier, D. Henderson, Z. Janas, R. Kirchner, I. Mukha, E. Roeckl, K. Schmidt, and J. Zylicz, Phys. Rev. C **69**, 015502 (2004).
[39] K. Blaum, G. Audi, D. Beck, G. Bollen, C. Guenaut, P. Delahaye, F. Herfurth, A. Kellerbauer, H.-J. Kluge, D. Lunney, D. Rodriguez, S. Schwarz, L. Schweikhard, C. Weber, and C. Yazidjian, Nucl. Phys. A **746**, 305c (2004).
[40] B. Blank *et al.*, Eur. Phys. J. A **44**, 363 (2010).
[41] R. O. Bondelid and J. W. Butler, Nucl. Phys. **53**, 618 (1964).
[42] S. A. Brindhaban and P. H. Barker, Phys. Rev. C **49**, 2401 (1994); reference replaces earlier conference proceedings from the same laboratory.
[43] J. W. Butler and R. O. Bondelid, Phys. Rev. **121**, 1770 (1961).
[44] R. H. Burch, C. A. Gagliardi, and R. E. Tribble, Phys. Rev. C **38**, 1365 (1988).
[45] J. T. Burke, P. A. Vetter, S. J. Freedman, B. K. Fujikawa, and W. T. Winter, Phys. Rev. C **74**, 025501 (2006)
[46] G. Canchel, B. Blank, M. Chartier, F. Delalee, P. Dendooven, C. Dossat, J. Giovinazzo, J. Huikari, A. S. Lalleman, M. J. Lopez Jimenez, V. Madec, J. L. Pedroza, H. Penttila, and J. C. Thomas, Eur. Phys. J. A **23**, 409 (2005).
[47] N. M. Chaudri, Fizika **16**(3), 297 (1984).
[48] L. Chen, J. C. Hardy, M. Bencomo, V. Horvat, N. Nica, and H. I. Park, Nucl. Instrum. Methods Phys. Res., Sect. A **728**, 81 (2013).
[49] G. J. Clark, J. M. Freeman, D. C. Robinson, J. S. Ryder, W. E. Burcham, and G. T. A. Squier, Nucl. Phys. A **215**, 429 (1973); this reference replaces the half-life value in Phys. Lett. B **35**, 503 (1971).
[50] C. N. Davids, in *Atomic Masses and Fundamental Constants 6*, edited by J. A. Nolen and W. Benenson (Plenum, New York, 1980), p. 419.
[51] W. W. Daehnick and R. D. Rosa, Phys. Rev. C **31**, 1499 (1985).
[52] P. De Wit and C. Van der Leun, Phys. Lett. B **30**, 639 (1969).
[53] R. M. DelVecchio and W. W. Daehnick, Phys. Rev. C **17**, 1809 (1978).
[54] M. A. van Driel, H. Klijnman, G. A. P. Engelbertink, H. H. Eggebhuisen, and J. A. J. Hermans, Nucl. Phys. A **240**, 98 (1975).
[55] R. Dunlop *et al.*, Phys. Rev. C **88**, 045501 (2013).
[56] P. M. Endt, Nucl. Phys. A **521**, 1 (1990).
[57] P. M. Endt, Nucl. Phys. A **633**, 1 (1998).
[58] T. Eronen, V. Elomaa, U. Hager, J. Hakala, A. Jokinen, A. Kankainen, I. Moore, H. Penttila, S. Rahaman, S. Rinta-Antila, A. Saastamoinen, T. Sonoda, J. Aysto, A. Bey, B. Blank, G. Canchel, C. Dossat, J. Giovinazzo, I. Matea, and N. Adimi, Phys. Lett. B **636**, 191 (2006).
[59] T. Eronen, V. Elomaa, U. Hager, J. Hakala, A. Jokinen, A. Kankainen, I. Moore, H. Penttila, S. Rahaman, J. Rissanen, A. Saastamoinen, T. Sonoda, J. Aysto, J. C. Hardy, and V. S. Kolhinen, Phys. Rev. Lett. **97**, 232501 (2006).
[60] T. Eronen, V.-V. Elomaa, U. Hager, J. Hakala, J. C. Hardy, A. Jokinen, A. Kankainen, I. D. Moore, H. Penttila, S. Rahaman, S. Rinta-Antila, J. Rissanen, A. Saastamoinen, T. Sonoda, C. Weber, and J. Aysto, Phys. Rev. Lett. **100**, 132502 (2008).
[61] T. Eronen, V.-V. Elomaa, U. Hager, J. Hakala, A. Jokinen, A. Kankainen, T. Kessler, I. D. Moore, S. Rahaman, J. Rissanen, C. Weber, and J. Aysto, Phys. Rev. C **79**, 032802(R) (2009).
[62] T. Eronen, V.-V. Elomaa, J. Hakala, J. C. Hardy, A. Jokinen, I. D. Moore, M. Reponen, J. Rissanen, A. Saastamoinen, C. Weber, and J. Aysto, Phys. Rev. Lett. **103**, 252501 (2009).
[63] T. Eronen, D. Gorelov, J. Hakala, J. C. Hardy, A. Jokinen, A. Kankainen, V. S. Kolhinen, I. D. Moore, H. Penttila, M. Reponen, J. Rissanen, A. Saastamoinen, and J. Aysto, Phys. Rev. C **83**, 055501 (2011).
[64] S. Ettenauer, M. C. Simon, A. T. Gallant, T. Brunner, U. Chowdhury, V. V. Simon, M. Brodeur, A. Chaudhuri, E. Mané, C. Andreoiu, G. Audi, J. R. Crespo López-Urrutia, P. Delheij, G. Gwinner, A. Lapierre, D. Lunney, M. R. Pearson, R. Ringle, J. Ullrich, and J. Dilling, Phys. Rev. Lett. **107**, 272501 (2011).
[65] T. Faestermann, R. Hertenberger, H.-F. Wirth, R. Krucken, M. Mahgoub, and P. Maier-Komor, Eur. Phys. J. A **42**, 339 (2009).
[66] P. Finlay *et al.*, Phys. Rev. C **78**, 025502 (2008); the branching-ratio result in this reference replaces the result reported in B. Hyland *et al.*, Phys. Rev. Lett. **97**, 102501 (2006).
[67] P. Finlay *et al.*, Phys. Rev. Lett. **106**, 032501 (2011).

[68] P. Finlay *et al.*, Phys. Rev. C **85**, 055501 (2012).

[69] G. Frick, A. Gallmann, D. E. Alburger, D. H. Wilkinson, and J. P. Coffin, Phys. Rev. **132**, 2169 (1963).

[70] J. M. Freeman, G. Murray, and W. E. Burcham, Phys. Lett. **17**, 317 (1965).

[71] J. M. Freeman, J. G. Jenkin, G. Murray, D. C. Robinson, and W. E. Burcham, Nucl. Phys. A **132**, 593 (1969); this reference replaces the half-life values in J. M. Freeman, J. G. Jenkin, G. Murray, and W. E. Burcham, Phys. Rev. Lett. **16**, 959 (1966).

[72] J. M. Freeman, R. J. Petty, S. D. Hoath, G. T. A. Squier, and W. E. Burcham, Phys. Lett. B **53**, 439 (1975).

[73] B. K. Fujikawa, S. J. Asztalos, R. M. Clark, M. A. Deleplanque-Stephens, P. Fallon, S. J. Freeman, J. P. Greene, I.-Y. Lee, L. J. Lising, A. O. Macchiavelli, R. W. MacLeod, J. C. Reich, M. A. Rowe, S.-Q. Shang, F. S. Stephens, and E. G. Wasserman, Phys. Lett. B **449**, 6 (1999).

[74] A. Gallmann, E. Aslanides, F. Jundt, and E. Jacobs, Phys. Rev. **186**, 1160 (1969).

[75] M. Gaelens, J. Andrzejewski, J. Camps, P. Decrock, M. Huyse, K. Kruglov, W. F. Mueller, A. Piechaczek, N. Severijns, J. Szerypo, G. Vancraeynest, P. Van Duppen, and J. Wauters, Eur. Phys. J. A **11**, 413 (2001).

[76] S. George, S. Baruah, B. Blank, K. Blaum, M. Breitenfeldt, U. Hager, F. Herfurth, A. Herlert, A. Kellerbauer, H.-J. Kluge, M. Kretzschmar, D. Lunney, R. Savreux, S. Schwarz, L. Schweikhard, and C. Yazidjian, Phys. Rev. Lett. **98**, 162501 (2007).

[77] S. George, G. Audi, B. Blank, K. Blaum, M. Breitenfeldt, U. Hager, F. Herfurth, A. Herlert, A. Kellerbauer, H.-J. Kluge, M. Kretzschmar, D. Lunney, R. Savreux, S. Schwarz, L. Schweikhard, and C. Yazidjian, Europhys. Lett. **82**, 50005 (2008).

[78] H. J. Gils, D. Flothmann, R. Loehken, and W. Wiesner, Nucl. Instrum. Methods **105**, 179 (1972).

[79] D. R. Goosman and D. E. Alburger, Phys. Rev. C **5**, 1893 (1972); the branching-ratio upper limit set in this reference is considered to replace the much higher value reported by D. R. Brown, S. M. Ferguson, and D. H. Wilkinson, Nucl. Phys. A **135**, 159 (1969).

[80] G. F. Grinyer *et al.*, Phys. Rev. C **76**, 025503 (2007).

[81] G. F. Grinyer *et al.*, Phys. Rev. C **77**, 015501 (2008).

[82] G. F. Grinyer, G. C. Ball, H. Bouzomita, S. Ettenauer, P. Finlay, A. B. Garnsworthy, P. E. Garrett, K. L. Green, G. Hackman, J. R. Leslie, C. J. Pearson, E. T. Rand, C. S. Sumithrarachchi, C. E. Svensson, J. C. Thomas, S. Triambak, and S. J. Williams, Phys. Rev. C **87**, 045502 (2013); this reference replaces the half-life value in Ref. [80].

[83] G. I. Harris and A. K. Hyder, Phys. Rev. **157**, 958 (1967).

[84] M. Hagen, K. H. Maier, and R. Michaelsen, Phys. Lett. B **26**, 432 (1968).

[85] J. C. Hardy and D. E. Alburger, Phys. Lett. B **42**, 341 (1972).

[86] J. C. Hardy, H. Schmeing, J. S. Geiger, and R. L. Graham, Nucl. Phys. A **223**, 157 (1974); this reference replaces results in J. C. Hardy, H. Schmeing, J. S. Geiger, R. L. Graham, and I. S. Towner, Phys. Rev. Lett. **29**, 1027 (1972).

[87] J. C. Hardy, H. R. Andrews, J. S. Geiger, R. L. Graham, J. A. Macdonald, and H. Schmeing, Phys. Rev. Lett. **33**, 1647 (1974).

[88] J. C. Hardy, H. Schmeing, W. Benenson, G. M. Crawley, E. Kashy, and H. Nann, Phys. Rev. C **9**, 252 (1974).

[89] J. C. Hardy, G. C. Ball, J. S. Geiger, R. L. Graham, J. A. Macdonald, and H. Schmeing, Phys. Rev. Lett. **33**, 320 (1974); the value for the ^{46}V Q_{EC} value from this reference was later withdrawn by J. C. Hardy and I. S. Towner, in *Atomic Masses and Fundamental Constants 5*, edited by J. H. Sanders and A. H. Wapstra (Plenum, New York, 1976), p. 66.

[90] J. C. Hardy, H. Schmeing, J. S. Geiger, and R. L. Graham, Nucl. Phys. A **246**, 61 (1975); this reference replaces results in J. C. Hardy, H. Schmeing, J. S. Geiger, R. L. Graham, and I. S. Towner, Phys. Rev. Lett. **29**, 1027 (1972).

[91] E. Hagberg, V. T. Koslowsky, J. C. Hardy, I. S. Towner, J. G. Hykawy, G. Savard, and T. Shinozuka, Phys. Rev. Lett. **73**, 396 (1994); uncertainties on the Gamow-Teller decays observed from ^{46}V and ^{50}Mn did not appear in this reference but have been derived from the original data and added here.

[92] P. D. Harty, N. S. Bowden, P. H. Barker, and P. A. Amundsen, Phys. Rev. C **58**, 821 (1998).

[93] J. C. Hardy and I. S. Towner, Phys. Rev. Lett. **88**, 252501 (2002).

[94] J. C. Hardy, V. E. Iacob, M. Sanchez-Vega, R. G. Neilson, A. Azhari, C. A. Gagliardi, V. E. Mayes, X. Tang, L. Trache, and R. E. Tribble, Phys. Rev. Lett. **91**, 082501 (2003).

[95] D. L. Hendrie and J. B. Gerhart, Phys. Rev. **121**, 846 (1961).

[96] A. M. Hernandez and W. W. Daehnick, Phys. Rev. C **24**, 2235 (1981).

[97] A. M. Hernandez and W. W. Daehnick, Phys. Rev. C **25**, 2957 (1982).

[98] R. G. Helmer and C. van der Leun, Nucl. Instrum. Methods Phys. Res., Sect. A **450**, 35 (2000).

[99] F. Herfurth, J. Dilling, A. Kellerbauer, G. Audi, D. Beck, G. Bollen, H.-J. Kluge, D. Lunney, R. B. Moore, C. Scheidenberger, S. Schwarz, G. Sikler, and J. Szerypo (Isolde Collaboration), Phys. Rev. Lett. **87**, 142501 (2001).

[100] F. Herfurth, A. Kellerbauer, F. Ames, G. Audi, D. Beck, K. Blaum, G. Bollen, O. Engels, H.-J. Kluge, D. Lunney, R. B. Moore, O. Oinonen, E. Sauvan, C. Scheidenberger, S. Schwarz, G. Sikler, and C. Weber, Eur. Phys. J. A **15**, 17 (2002).

[101] I. Hofmann, Acta Phys. Aust. **18**, 309 (1964).

[102] S. D. Hoath, R. J. Petty, J. M. Freeman, G. T. A. Squier, and W. E. Burcham, Phys. Lett. B **51**, 345 (1974).

[103] P. Hungerford and H. H. Schmidt, Nucl. Instrum. Methods **192**, 609 (1982).

[104] B. C. Hyman, V. E. Iacob, A. Azhari, C. A. Gagliardi, J. C. Hardy, V. E. Mayes, R. G. Nielson, M. Sanchez-Vega, X. Tang, L. Trache, and R. E. Tribble, Phys. Rev. C **68**, 015501 (2003).

[105] B. Hyland, D. Melconian, G. C. Ball, J. R. Leslie, C. E. Svensson, P. Bricault, E. Cunningham, M. Dombsky, G. F. Grinyer, G. Hackman, K. Koopmans, F. Sarazin, M. A. Schumaker, H. C. Scraggs, M. B. Smith, and P. M. Walker, J. Phys. G: Nucl. Part. Phys. **31**, S1885 (2005).

[106] V. E. Iacob, J. C. Hardy, J. F. Brinkley, C. A. Gagliardi, V. E. Mayes, N. Nica, M. Sanchez-Vega, G. Tabacaru, L. Trache, and R. E. Tribble, Phys. Rev. C **74**, 055502 (2006).

[107] V. E. Iacob, J. C. Hardy, V. Golovko, J. Goodwin, N. Nica, H. I. Park, L. Trache, and R. E. Tribble, Phys. Rev. C **77**, 045501 (2008).

[108] V. E. Iacob, J. C. Hardy, A. Banu, L. Chen, V. V. Golovko, J. Goodwin, V. Horvat, N. Nica, H. I. Park, L. Trache, and R. E. Tribble, Phys. Rev. C **82**, 035502 (2010).

[109] P. D. Ingalls, J. C. Overley, and H. S. Wilson, Nucl. Phys. A **293**, 117 (1977).

[110] M. A. Islam, T. J. Kennett, S. A. Kerr, and W. V. Prestwich, Can. J. Phys. **58**, 168 (1980).

[111] C. Jewett, C. Baktash, D. Bardayan, J. Blackmon, K. Chipps, A. Galindo-Uribarri, U. Greife, C. Gross, K. Jones, F. Liang, J. Livesay, R. Kozub, C. Nesaraja, D. Radford, F. Sarazin, M. S. Smith, J. Thomas, and C.-H. Yu, Nucl. Instrum. Methods Phys. Res., Sect. B **261**, 945 (2007).

[112] M. J. Lopez Jimenez, B. Blank, M. Chartier, S. Czajkowski, P. Dessagne, G. de France, J. Giovinazzo, D. Karamanis, M. Lewitowicz, V. Maslov, C. Miehe, P. H. Regan, M. Stanoiu, and M. Wiescher, Phys. Rev. C **66**, 025803 (2002).

[113] R. W. Kavanagh, Nucl. Phys. A **129**, 172 (1969).

[114] A. Kellerbauer, G. Audi, D. Beck, K. Blaum, G. Bollen, C. Guenaut, F. Herfurth, A. Herlert, D. Lunney, H.-J. Kluge, S. Schwarz, L. Schweikhard, C. Weber, and C. Yazidjian, Phys. Rev. C **76**, 045504 (2007); this result for the mass of ^{74}Rb is the same as—but more clearly explained than—the result given in A. Kellerbauer, G. Audi, D. Beck, K. Blaum, G. Bollen, B. A. Brown, P. Delahaye, C. Guénaut, F. Herfurth, D. Lunney, H.-J. Kluge, S. Schwarz, L. Schweikhard, and C. Yazidjian, Phys. Rev. Lett. **93**, 072502 (2004).

[115] S. W. Kikstra, C. van der Leun, S. Raman, E. T. Jurney, and I. S. Towner, Nucl. Phys. A **496**, 429 (1989).

[116] S. W. Kikstra, Z. Guo, C. Van der Leun, P. M. Endt, S. Raman, Walkiewicz, J. W. Starner, E. T. Jurney, and I. S. Towner, Nucl. Phys. A **529**, 39 (1991).

[117] V. T. Koslowsky, E. Hagberg, J. C. Hardy, R. E. Azuma, E. T. H. Clifford, H. C. Evans, H. Schmeing, U. J. Schrewe, and K. S. Sharma, Nucl. Phys. A **405**, 29 (1983).

[118] V. T. Koslowsky, J. C. Hardy, E. Hagberg, R. E. Azuma, G. C. Ball, E. T. H. Clifford, W. G. Davies, H. Schmeing, U. J. Schrewe, and K. S. Sharma, Nucl. Phys. A **472**, 419 (1987); the ^{14}O-^{26}Al^m Q_{EC}-value-difference result reported in this reference replaces an earlier value given in V. T. Koslowsky, J. C. Hardy, R. E. Azuma, G. C. Ball, E. T. H. Clifford, W. G. Davies, E. Hagberg, H. Schmeing, U. J. Schrewe, and K. S. Sharma, Phys. Lett. B **119**, 57 (1982).

[119] V. T. Koslowsky, E. Hagberg, J. C. Hardy, G. Savard, H. Schmeing, K. S. Sharma, and X. J. Sun, Nucl. Instrum. Methods A **401**, 289 (1997).

[120] V. T. Koslowsky, E. Hagberg, J. C. Hardy, H. Schmeing, and I. S. Towner, Nucl. Phys. A **624**, 293 (1997).

[121] M. A. Kroupa, S. J. Freeman, P. H. Barker, and S. M. Ferguson, Nucl. Instrum. Methods Phys. Res., Sect. A **310**, 649 (1991).

[122] T. Kurtukian Nieto *et al.*, Phys. Rev. C **80**, 035502 (2009).

[123] A. A. Kwiatkowski, B. R. Barquest, G. Bollen, C. M. Campbell, R. Ferrer, A. E. Gehring, D. L. Lincoln, D. J. Morrissey, G. K. Pang, J. Savory, and S. Schwarz, Phys. Rev. C **81**, 058501 (2010).

[124] A. A. Kwiatkowski, A. Chaudhuri, U. Chowdhury, A. T. Gallant, T. D. Macdonald, B. E. Schultz, M. C. Simon, and J. Dilling, Ann. Phys. (Berlin) **525**, 529 (2013).

[125] A. T. Laffoley *et al.*, Phys. Rev. C **88**, 015501 (2013).

[126] K. G. Leach *et al.*, Phys. Rev. Lett. **100**, 192504 (2008).

[127] S. Lin, S. A. Brindhaban, and P. H. Barker, Phys. Rev. C **49**, 3098 (1994).

[128] P. V. Magnus, E. G. Adelberger, and A. Garcia, Phys. Rev. C **49**, R1755 (1994).

[129] I. Matea *et al.*, Eur. Phys. J. A **37**, 151 (2008); **38**, 247(E) (2008).

[130] W. R. McMurray, P. Van der Merwe, and I. J. Van Heerden, Nucl. Phys. A **92**, 401 (1967).

[131] R. G. Miller and R. W. Kavanagh, Nucl. Phys. A **94**, 261 (1967).

[132] C. E. Moss, C. Detraz, and C. S. Zaidins, Nucl. Phys. A **174**, 408 (1971).

[133] M. Mukherjee, A. Kellerbauer, D. Beck, K. Blaum, G. Bollen, F. Carrel, P. Delahaye, J. Dilling, S. George, C. Guenaut, F. Herfurth, A. Herlert, H.-J. Kluge, U. Koster, D. Lunney, S. Schwarz, L. Schweikhard, and C. Yazidjian, Phys. Rev. Lett. **93**, 150801 (2004).

[134] Y. Nagai, K. Kunihiro, T. Toriyama, S. Harada, Y. Torii, A. Yoshida, T. Nomura, J. Tanaka, and T. Shinozuka, Phys. Rev. C **43**, R9 (1991).

[135] J. A. Nolen, G. Hamilton, E. Kashy, and I. D. Proctor, Nucl. Instrum. Methods **115**, 189 (1974).

[136] M. Oinonen *et al.*, Phys. Lett. B **511**, 145 (2001).

[137] R. A. Paddock, Phys. Rev. C **5**, 485 (1972).

[138] A. Parikh, J. A. Caggiano, C. Deibel, J. P. Greene, R. Lewis, P. D. Parker, and C. Wrede, Phys. Rev. C **71**, 055804 (2005).

[139] H. I. Park, J. C. Hardy, V. E. Iacob, A. Banu, L. Chen, V. V. Golovko, J. Goodwin, V. Horvat, N. Nica, E. Simmons, L. Trache, and R. E. Tribble, Phys. Rev. C **84**, 065502 (2011).

[140] H. I. Park, J. C. Hardy, V. E. Iacob, L. Chen, J. Goodwin, N. Nica, E. Simmons, L. Trache, and R. E. Tribble, Phys. Rev. C **85**, 035501 (2012).

[141] H. I. Park, J. C. Hardy, V. E. Iacob, M. Bencomo, L. Chen, V. Horvat, N. Nica, B. T. Roeder, E. Simmons, R. E. Tribble, and I. S. Towner, Phys. Rev. Lett. **112**, 102502 (2014).

[142] A. Piechaczek, E. F. Zganjar, G. C. Ball, P. Bricault, J. M. D'Auria, J. C. Hardy, D. F. Hodgson, V. Iacob, P. Klages, W. D. Kulp, J. R. Leslie, M. Lipoglavsek, J. A. Macdonald, H.-B. Mak, D. M. Moltz, G. Savard, J. von Schwarzenberg, C. E. Svensson, I. S. Towner, and J. L. Wood, Phys. Rev. C **67**, 051305(R) (2003); the branching-ratio results from this measurement are considered to replace the contradictory upper limit set in an earlier less-precise measurement [136].

[143] F. W. Prosser, G. U. Din, and D. D. Tolbert, Phys. Rev. **157**, 779 (1967).

[144] W. V. Prestwich and T. J. Kennett, Can. J. Phys. **68**, 261 (1990); **68**, 1352(E) (1990).

[145] S. Raman, E. T. Jurney, D. A. Outlaw, and I. S. Towner, Phys. Rev. C **27**, 1188 (1983).

[146] J. P. L. Reinecke, F. B. Waanders, P. Oberholtzer, P. J. C. Janse van Rensburg, J. A. Cilliers, J. J. A. Smit, M. A. Meyer, and P. M. Endt, Nucl. Phys. A **435**, 333 (1985).

[147] R. Ringle, T. Sun, G. Bollen, D. Davies, M. Facina, J. Huikari, E. Kwan, D. J. Morrissey, A. Prinke, J. Savory, P. Schury, S. Schwarz, and C. S. Sumithrarachchi, Phys. Rev. C **75**, 055503 (2007); this result is the same as that appearing in G. Bollen, D. Davies, M. Facina, J. Huikari, E. Kwan, P. A. Lofy, D. J. Morrissey, A. Prinke, R. Ringle, J. Savory, P. Schury, S. Schwarz, C. Sumithrarachchi, T. Sun, and L. Weissman, Phys. Rev. Lett. **96**, 152501 (2006).

[148] M. L. Roush, L. A. West, and J. B. Marion, Nucl. Phys. A **147**, 235 (1970).

[149] D. C. Robinson, J. M. Freeman, and T. T. Thwaites, Nucl. Phys. A **181**, 645 (1972); this reference replaces the ^{10}C branching ratio from J. M. Freeman, J. G. Jenkin, and G. Murray, *ibid.* **124**, 393 (1969).

[150] D. C. Robinson and P. H. Barker, Nucl. Phys. A **225**, 109 (1974).

[151] C. Rolfs, W. S. Rodney, S. Durrance, and H. Winkler, Nucl. Phys. A **240**, 221 (1975).

[152] D. Rodriguez, G. Audi, J. Aysto, D. Beck, K. Blaum, G. Bollen, F. Herfurth, A. Jokinen, A. Kellerbauer, H.-J. Kluge, V. S. Kohlinen, M. Oinonen, E. Sauvan, and S. Schwarz, Nucl. Phys. A **769**, 1 (2006); this result for the mass of ^{74}Kr is the same as—but more clearly explained than—the result given in A. Kellerbauer, A. Kellerbauer, G. Audi, D. Beck, K. Blaum, G. Bollen, B. A. Brown, P. Delahaye, C. Guénaut, F. Herfurth, D. Lunney, H.-J. Kluge, S. Schwarz, L. Schweikhard, and C. Yazidjian, Phys. Rev. Lett. **93**, 072502 (2004).

[153] J. S. Ryder, G. J. Clark, J. E. Draper, J. M. Freeman, W. E. Burcham, and G. T. A. Squier, Phys. Lett. B **43**, 30 (1973).

[154] A. Rytz, At. Data Nucl. Data Tables **47**, 205 (1991).

[155] A. M. Sandorfi, C. J. Lister, D. E. Alburger, and E. K. Warburton, Phys. Rev. C **22**, 2213 (1980).

[156] G. Savard, A. Galindo-Uribarri, E. Hagberg, J. C. Hardy, V. T. Koslowsky, D. C. Radford, and I. S. Towner, Phys. Rev. Lett. **74**, 1521 (1995).

[157] G. Savard, J. A. Clark, F. Buchinger, J. E. Crawford, S. Gulick, J. C. Hardy, A. A. Hecht, V. E. Iacob, J. K. P. Lee, A. F. Levand, B. F. Lundgren, N. D. Scielzo, K. S. Sharma, I. Tanihata, I. S. Towner, W. Trimble, J. C. Wang, Y. Wang, and Z. Zhou, Phys. Rev. C **70**, 042501(R) (2004).

[158] G. Savard, F. Buchinger, J. A. Clark, J. E. Crawford, S. Gulick, J. C. Hardy, A. A. Hecht, J. K. P. Lee, A. F. Levand, N. D. Scielzo, H. Sharma, K. S. Sharma, I. Tanihata, A. C. C. Villari, and Y. Wang, Phys. Rev. Lett. **95**, 102501 (2005).

[159] J. Savory, P. Schury, C. Bachelet, M. Block, G. Bollen, M. Facina, C. M. Folden, III, C. Guénaut, E. Kwan, A. A. Kwiatkowski, D. J. Morrissey, G. K. Pang, A. Prinke, R. Ringle, H. Schatz, S. Schwarz, and C. S. Sumithrarachchi, Phys. Rev. Lett. **102**, 132501 (2009).

[160] P. Schury, C. Bachelet, M. Block, G. Bollen, D. A. Davies, M. Facina, C. M. Folden, C. Guénaut, J. Huikari, E. Kwan, A. Kwiatkowski, D. J. Morrissey, R. Ringle, G. K. Pang, A. Prinke, J. Savory, H. Schatz, S. Schwarz, C. S. Sumithrarachchi, and T. Sun, Phys. Rev. C **75**, 055801 (2007).

[161] R. J. Scott, G. J. O'Keefe, M. N. Thompson, and R. P. Rassool, Phys. Rev. C **84**, 024611 (2011).

[162] J. C. Sens, A. Pape, and R. Armbruster, Nucl. Phys. A **199**, 241 (1973).

[163] D. Seweryniak, P. J. Woods, M. P. Carpenter, T. Davinson, R. V. F. Janssens, D. G. Jenkins, T. Lauritsen, C. J. Lister, C. Ruiz, J. Shergur, S. Sinha, and A. Woehr, Phys. Rev. Lett. **94**, 032501 (2005).

[164] R. Sherr, J. B. Gerhart, H. Horie, and W. F. Hornyak, Phys. Rev. **100**, 945 (1955).

[165] G. S. Sidhu and J. B. Gerhart, Phys. Rev. **148**, 1024 (1966).

[166] J. Singh, Indian J. Pure Appl. Phys. **10**, 289 (1972).

[167] J. Souin, T. Eronen, P. Ascher, L. Audirac, J. Aysto, B. Blank, V.-V. Elomaa, J. Giovinazzo, J. Hakala, A. Jokinen, V. S. Kolhinen, P. Karvonen, I. D. Moore, S. Rahaman, J. Rissanen, A. Saastamoinen, and J. C. Thomas, Eur. Phys. J. A **47**, 40 (2011).

[168] G. T. A. Squier, W. E. Burcham, J. M. Freeman, R. J. Petty, S. D. Hoath, and J. S. Ryder, Nucl. Phys. A **242**, 62 (1975).

[169] V. T. Takau, M. N. Thompson, R. J. Scott, R. P. Rassool, and G. J. O'Keefe, Rad. Phys. Chem. **81**, 1669 (2012).

[170] D. R. Tilley, H. R. Weller, C. M. Cheves, and R. M. Chasteler, Nucl. Phys. A **595**, 1 (1995).

[171] N. R. Tolich, P. H. Barker, P. D. Harty, and P. A. Amundsen, Phys. Rev. C **67**, 035503 (2003).

[172] I. S. Towner and J. C. Hardy, Phys. Rev. C **72**, 055501 (2005).

[173] H. Vonach, P. Glaessel, E. Huenges, P. Maier-Komor, H. Roesler, H. J. Scheerer, H. Paul, and D. Semrad, Nucl. Phys. A **278**, 189 (1977).

[174] F. B. Waanders, J. P. L. Reinecke, H. N. Jacobs, J. J. A. Smit, M. A. Meyer, and P. M. Endt, Nucl. Phys. A **411**, 81 (1983).

[175] T. A. Walkiewicz, S. Raman, E. T. Jurney, J. W. Starner, and J. E. Lynn, Phys. Rev. C **45**, 1597 (1992).

[176] M. Wang, G. Audi, A. H. Wapstra, F. G. Kondev, M. MacCormick, X. Xu, and B. Pfeiffer, Chin. Phys. C **36**, 1603 (2012).

[177] H. Wenninger, J. Stiewe, and H. Leutz, Nucl. Phys. A **109**, 561 (1968).

[178] R. E. White and H. Naylor, Nucl. Phys. A **276**, 333 (1977).

[179] R. E. White, H. Naylor, P. H. Barker, D. M. J. Lovelock, and R. M. Smythe, Phys. Lett. B **105**, 116 (1981).

[180] R. E. White, P. H. Barker, and D. M. J. Lovelock, Metrologea **21**, 193 (1985).

[181] D. H. Wilkinson and D. E. Alburger, Phys. Rev. C **13**, 2517 (1976).

[182] D. H. Wilkinson, A. Gallmann, and D. E. Alburger, Phys. Rev. C **18**, 401 (1978).

[183] H. S. Wilson, R. W. Kavanagh, and F. M. Mann, Phys. Rev. C **22**, 1696 (1980).

[184] F. Zijderhand, R. C. Markus, and C. van der Leun, Nucl. Phys. A **466**, 280 (1987).

[185] K. A. Olive *et al.* [Particle Data Group], Chin. Phys. C **38**, 090001 (2014).

[186] W. J. Marciano and A. Sirlin, Phys. Rev. Lett. **96**, 032002 (2006).

[187] A. Sirlin, Phys. Rev. **164**, 1767 (1967).

[188] A. Sirlin and R. Zucchini, Phys. Rev. Lett. **57**, 1994 (1986).

[189] W. Jaus and G. Rasche, Phys. Rev. D **35**, 3420 (1987).

[190] A. Sirlin, Phys. Rev. D **35**, 3423 (1987).

[191] A. Czarnecki, W. J. Marciano, and A. Sirlin, Phys. Rev. D **70**, 093006 (2004).

[192] I. S. Towner and J. C. Hardy, Phys. Rev. C **77**, 025501 (2008).

[193] M. MacCormick and G. Audi, Nucl. Phys. A **925**, 61 (2014); **925**, 296 (2014).

[194] G. Audi, F. G. Kondev, M. Wang, B. Pfeiffer, X. Sun, J. Blachot, and M. MacCormick, Chin. Phys. C **36**, 1157 (2012).

[195] H. De Vries, C. W. De Jager, and C. De Vries, At. Data Nucl. Data Tables **36**, 495 (1987).

[196] I. S. Towner and J. C. Hardy, Phys. Rev. C **66**, 035501 (2002).

[197] I. Angeli, At. Data Nucl. Data Tables **87**, 185 (2004).

[198] E. Mané, A. Voss, J. A. Behr, J. Billowes, T. Brunner, F. Buchinger, J. E. Crawford, J. Dilling, S. Ettenauer, C. D. P. Levy, O. Shelbaya, and M. R. Pearson, Phys. Rev. Lett. **107**, 212502 (2011).

[199] W. E. Ormand and B. A. Brown, Phys. Rev. Lett. **62**, 866 (1989).

[200] J. Le Bloas, L. Bonneau, P. Quentin, and J. Bartel, Int. J. Mod. Phys. E **20**, 274 (2011).

[201] H. Sagawa, N. Van Giai, and T. Suzuki, Phys. Rev. C **53**, 2163 (1996).
[202] H. Liang, N. V. Giai, and J. Meng, Phys. Rev. C **79**, 064316 (2009).
[203] Z. X. Li, J. M. Yao, and H. Chen, Sci. China Phys. Mech. Astron. **54**, 1131 (2011).
[204] N. Auerbach, Phys. Rev. C **79**, 035502 (2009).
[205] V. Rodin, Phys. Rev. C **88**, 064318 (2013).
[206] W. Satula, J. Dobaczewski, W. Nazarewicz, and T. R. Werner, Phys. Rev. C **86**, 054316 (2012).
[207] M. Beiner, H. Flocard, N. van Giai, and P. Quentin, Nucl. Phys. A **238**, 29 (1975).
[208] I. S. Towner and J. C. Hardy, Phys. Rev. C **82**, 065501 (2010).
[209] V. Tishchenko *et al.* (MuLan Collaboration), Phys. Rev. D **87**, 052003 (2013).
[210] I. S. Towner and J. C. Hardy, in *Symmetries and Fundamental Interactions in Nuclei*, edited by W. C. Haxton and E. M. Henley (World-Scientific, Singapore, 1995), pp. 183–249.
[211] I. S. Towner and J. C. Hardy, in *Proceedings of the V International WEIN Symposium: Physics Beyond the Standard Model, Santa Fe, NM 1998*, edited by P. Herzeg, C. M. Hoffman, and H. V. Klapdor-Kleingrothaus (World-Scientific, Singapore, 1999), pp. 338–359.
[212] M. Antonelli *et al.* [FlaviaNet Working Group on Kaon Decays], Eur. Phys. J. C **69**, 399 (2010).
[213] M. Moulson, *Proceedings of the 8th International Workshop on the CKM Unitarity Triangle (CKM 14), Vienna* (2014), arXiv:1411.5252, and private communication.
[214] S. Aoki *et al.* [Flavour Lattice Averaging Group (FLAG)], arXiv:1310.8555v4.
[215] A. Bazavov *et al.* [FermiLab Lattice and MILC collaborations], Phys. Rev. Lett. **112**, 112001 (2014).
[216] A. Bazavov *et al.* [FermiLab Lattice and MILC collaborations], Phys. Rev. D **90**, 074509 (2014).
[217] E. Blucher and W. J. Marciano, V_{ud}, V_{us}, *the Cabibbo Angle, and CKM Unitarity*, minireview for Particle Data Group. See Ref. [185] page 933.
[218] J. D. Jackson, S. B. Treiman, and H. W. Wyld, Jr., Phys. Rev. **106**, 517 (1957).
[219] A. Gorelov *et al.*, Phys. Rev. Lett. **94**, 142501 (2005).
[220] O. Naviliat-Cuncic and M. González-Alonso, Ann. Phys. (Berlin) **525**, 600 (2013).
[221] H. Behrens and W. Bühring, *Electron Radial Wave Functions and Nuclear Beta-decay* (Clarendon Press, Oxford, U.K., 1982).